3. SITE 554[1]

Shipboard Scientific Party[2]

HOLE 554

Date occupied: 27 August 1981

Date departed: 28 August 1981

Time on hole: 26.5 hr.

Position (latitude; longitude): 56°17.41'N; 23°31.69'W

Water depth (sea level; corrected m, echo-sounding): 2574

Water depth (rig floor; corrected m, echo-sounding): 2584

Bottom felt (m, drill pipe): 2584

Penetration (m): 76

Number of cores: 8

Total length of cored section (m): 76

Total core recovered (m): 53.76

Core recovery (%): 71

Oldest sediment cored:
Depth sub-bottom (m): 76
Nature: Nannofossil-foraminiferal ooze
Age: late Miocene
Measured velocity (km/s): 1.5

Principal results: See Chapter 1, Introduction and Explanatory Notes.

HOLE 554A

Date occupied: 28 August 1981

Date departed: 29 August 1981

Time on hole: 41 hr., 7 min.

Position (latitude; longitude): 56°17.4'N; 23°31.69'W

Water depth (sea level; corrected m, echo-sounding): 2574

Water depth (rig floor; corrected m, echo-sounding): 2584

Bottom felt (m, drill pipe): 2584

Penetration (m): 209

Number of cores: 14

Total length of cored section (m): 133 (washed 76 m)

Total core recovered (m): 29.52

Core recovery (%): 22

Oldest sediment cored:
Depth sub-bottom (m): 126.6
Nature: Tuffaceous marlstone
Age: early Eocene
Measured velocity (km/s): 2.3

Basement:
Depth sub-bottom (m): 126.75
Nature: Basaltic lava
Velocity range (km/s): 5

Principal results: See Chapter 1, Introduction and Explanatory Notes.

BACKGROUND AND OBJECTIVES

Site 554 was drilled to examine the nature and origin of the outer high forming the western boundary of the suite of seaward dipping reflectors at the base of the Rockall Plateau. The high was located in the region of the possible continent–ocean transition shown by partial overlap of oldest Anomaly 24B with the high. The location of the site is shown in Figure 1.

Outer highs are thought to be a common feature of many passive margins (Scheupbach and Vail, 1980) and are typically found in the vicinity of the continent–ocean transition. The high has been identified on margins characterized by well-developed tilted and rotated fault blocks such as Goban Spur (Montadert, Roberts, et al., 1979) and Galicia Bank (Groupe Galice, 1979) as well as those associated with dipping reflectors such as the Rockall Plateau and Vøring Plateau (Hinz, 1981). The high has also been found off the east coast of the United States, where it is associated with the East Coast Magnetic Anomaly (Grow, et al., 1980). Comparable features seem to be present off southern Australia (Talwani, et al., 1979) and on the west margin of India (Naini, 1981), where the seismic velocity structure is distinctly different on the "landward" and "oceanic" sides of the high. Where the conjugate margin is present, a mirror image of the high seems to be present. Thus, the "outer high" observed off northwest Africa may be equivalent to the "high" off the east coast of the U.S. A similar but much less defined feature off East Greenland (Featherstone, et al., 1977; Roberts, unpubl.) may match the outer high west of Rockall Plateau. Little is known however of the nature and origin of the high. Dredging of a possible "outer high" west of Galicia Bank has yielded lherzolites of continental affinity (Boillot, et al., 1980), but drilling during Leg 80 of a similar feature at the foot of Goban Spur provided basalt (De Graciansky, pers. comm.).

Interpretation of the origin of the high has been based on the seismic stratigraphy of the sediments both on and around the high. Scheupbach and Vail (1980) interpret

[1] Roberts, D. G., Schnitker, D., et al., *Init. Repts. DSDP*, 81: Washington (U.S. Govt. Printing Office).

[2] David G. Roberts (Co-Chief Scientist), Institute of Oceanographic Sciences, Wormley, Godalming, Surrey, United Kingdom (present address: British Petroleum Co. Ltd., Britannic House, Moor Lane, London, United Kingdom); Detmar Schnitker (Co-Chief Scientist), Department of Oceanography, University of Maine, Walpole, Maine; Jan Backman, Geologiska Institutionen, Stockholms Universitet, Kungstensgaten 45, S-113 86 Stockholm, Sweden; Jack G. Baldauf, Paleontology and Stratigraphy Bureau, U.S. Geological Survey, Menlo Park, California; Alain Desprairies, Laboratoire de Géochimie des Roches Sédimentaires, Université de Paris XI, 91405 Orsay, France; Reiner Homrighausen, Laboratorium fur Erdolgewinnung, Deutsche Texaco AG, 3101 Wietze, Federal Republic of Germany; Paul Huddlestun, Georgia Geological Survey, Atlanta, Georgia; Alfred J. Kaltenback, Denver Research Center, Marathon Oil Company, Littleton, Colorado; John B. Keene, Deep Sea Drilling Project, Scripps Institution of Oceanography, La Jolla, California (present address: Department of Geology, University of Sydney, NSW, Australia); Klaus A. O. Krumsiek, Geologisches Institut, Bonn, Nussallee 8, D 53 Bonn 1, Federal Republic of Germany; Andrew C. Morton, British Geological Survey, Keyworth, United Kingdom; John W. Murray, Department of Geology, University of Exeter, Exeter, Devon, United Kingdom; Jean Westberg-Smith, Geological Research Division, Scripps Institute of Oceanography, La Jolla, California; Herman B. Zimmerman, Department of Civil Engineering, Union College, Schenectady, New York.

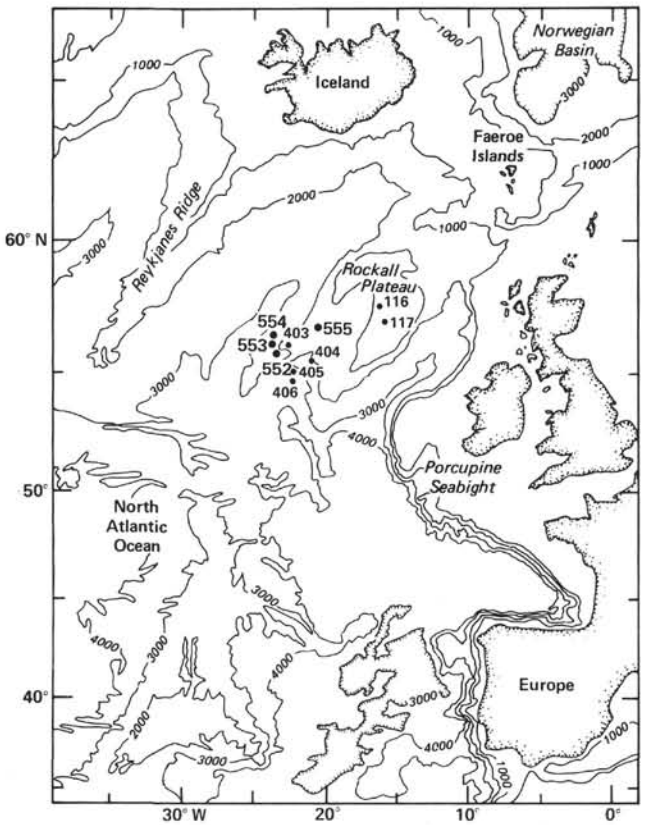

Figure 1. Northeast Atlantic bathymetry showing locations of Sites 552, 553, 554, 555, 403, 404, 405, 406, 116, and 117.

onlap of late phase rift sediments onto the high as evidence that it was a positive feature during the later stages of rifting. Landward progradation observed on the outer high of the Vøring Plateau may be supporting evidence that it was a positive feature during the later stages of rifting. In some cases, an oceanward dip of the flat surface of the high has been interpreted as oceanward tilting of a subaerial erosion surface during the postrift thermal subsidence of the margin (Vail, pers. comm., 1981).

The origin of the high appears to be directly related to the latest stages of rifting and the development of the continent–ocean transition. In this context, Vierbuchen et al. (1981) from theoretical considerations regard the high as having formed by a thermo-mechanical event that immediately preceded the formation of ocean crust and caused a narrow axial uplift within the rift graben. In their model, uplift of the outer high is considered to have resulted from rapidly accelerating extensional deformation in the ductile part of the lithosphere and a concurrent rise in mantle isotherms. At the rift axis, thinning of the brittle layer causes an initial subsidence but the acceleration of the strain rate in the ductile layers eventually propagates uplift. It is quite conceivable therefore that the outer high may represent the first formed ocean crust.

On Rockall Plateau (Fig. 2) an outer high can be followed nearly continuously for the length of the west margin (Roberts et al., 1979). The high varies in relief from north to south. In the north, the high is a prominent flat-topped, possibly subaerially eroded ridge that is parallel to the adjacent oceanic magnetic anomalies. Farther south, the high becomes more subdued and is covered by thin sediments. In all cases, however, the high seems to form the oceanward boundary of the dipping reflector sequence and is also shallower than the basalts forming the top of the dipping reflector sequences. In relation to the adjoining oceanic anomalies, the outer high lies at the transition from Anomaly 24B to the broad generally negative anomaly associated with the dipping reflector sequence (Jones and Roberts, 1975; Roberts et al., 1979). Figure 3, from another seismic profile across the margin, illustrates these relationships.

The control seismic profile (IFP-CEPM RH 115) shows a 15-km-wide high bounded oceanward by a steep slope where basement outcrops or is covered by thin sediments (Figs. 3 and 4). The basement of the high ostensibly merges with the adjoining oceanic basement within which impersistent dipping reflectors can be seen. On the high itself, thin (0.3 s) sediments are present. A sharp downward step occurring landward of the high separates it from the deeper top of the basalt sequence drilled at Hole 553A. The site was originally planned at the base of the oceanward slope of high. However, in view of the lack of sediments, it was decided to move the site to the crestal area of the high to benefit from the greater stratigraphic resolution potentially provided by the thicker sedimentary section above the crest of the high (Figs. 3 and 5).

The principal objective of Site 554 was to examine the origin of the outer high in relationship to the transition from rifting to spreading and the dipping reflectors drilled at Site 553. Within this broadly stated objective, the following specific problems were to be examined.

Nature of the outer high: Drilling was intended to penetrate the basement of the outer high to establish its nature (oceanic or transition), origin, and age in relation to the first anomaly (24B) recorded in the adjacent ocean crust.

Subsidence: Sediments overlying the high may contain a record of uplift and subsidence, thus enabling comparison of this history with that predicted for the ocean crust to the west and that found at Site 553 in the adjoining dipping reflector sequence. Information on the subsidence history might indirectly contribute to an assessment of the water depths in which the first oceanic crust formed.

Paleomagnetism: Paleomagnetic studies had the objective of establishing the age of the high in relation to the oceanic magnetic Anomaly 24B.

Heat-flow studies: Heat-flow measurements had the objective of providing a comparison with those expected for oceanic crust aged between 50 and 60 m.y.

Well logging: It was hoped to use the logging results to correlate the section above the basement with that found at Site 553.

Paleoceanography: Since the use of the hydraulic piston core (HPC) at Hole 553B had been a complete failure, an ancillary objective was to try to HPC the important Pliocene–Pleistocene section again.

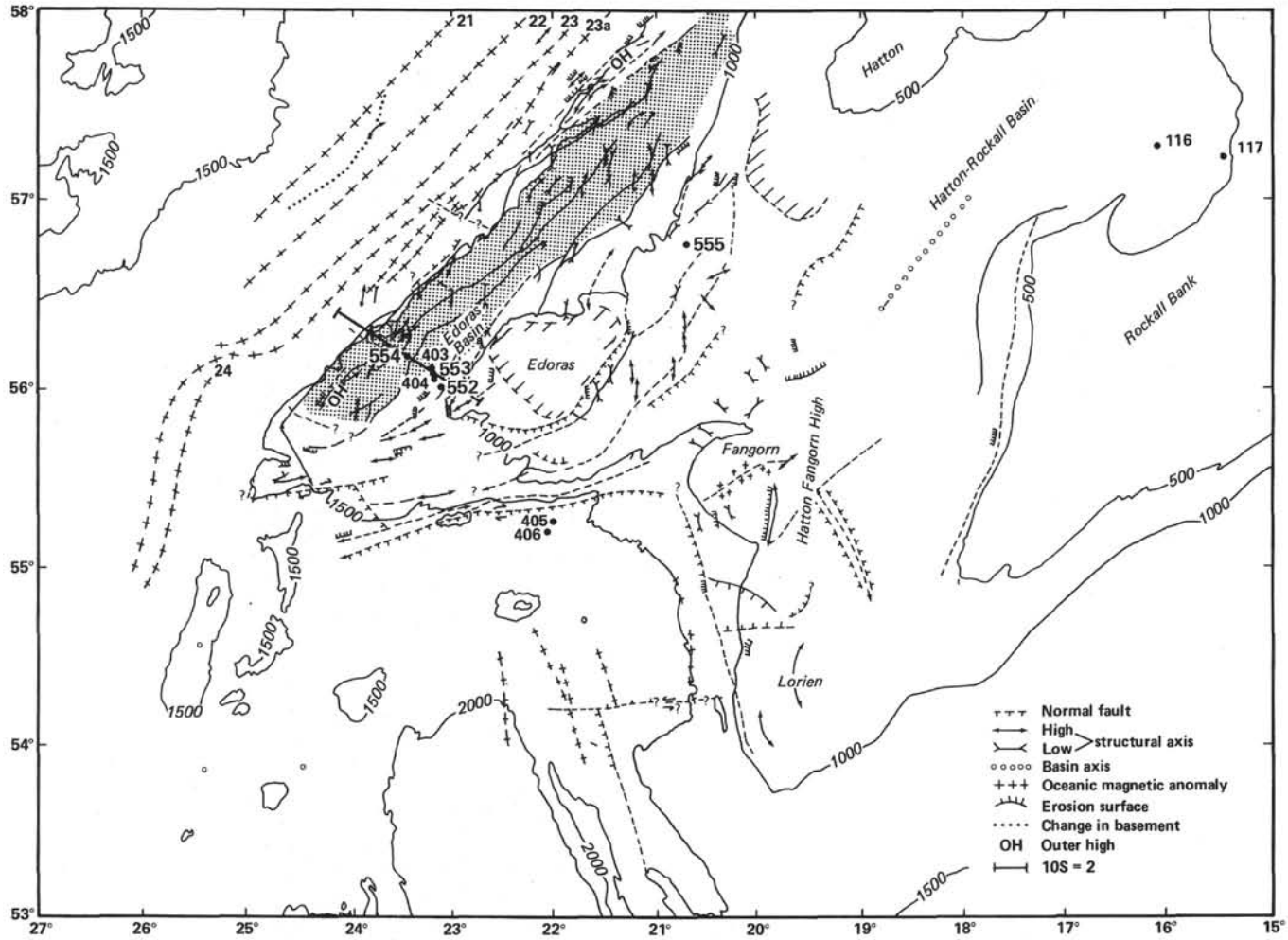

Figure 2. Principal structural elements of the southwestern Rockall Plateau based on seismic reflection profiles and magnetic data.

OPERATIONS

Following the two abortive attempts to HPC at Hole 553B, it was decided to abandon further attempts and to commence drilling at Site 554 situated on the outer high. After securing the rig floor, *Glomar Challenger* got underway for Site 554, streaming the seismic gear for the passage to Site 554. Course was initially set to the southwest to allow a seismic profile across the site to be made. Heavy seas and unreliable LORAN-C fixes made this impossible. At 0230Z (Fig. 6), course was set to the northwest to run along the control seismic profile IFP-CEPM 115 crossing Site 554. The site was crossed at 0403Z, but course was maintained until 0440Z in order to cross the oceanward foot of the outer high, thus checking the navigation. At this time, the *Glomar Challenger* altered course to return to the site, deploying the beacon at 0514Z. Navigation throughout the site approach was particularly difficult. Satellite fixes were sparse and the LORAN-C consistently offset from the OMEGA. The latter navaid proved surprisingly reliable, giving a fix only 0.2 n. mi. different from the satellite fix fortuitously observed at the beacon drop. At 0630Z, 27 August, *Glomar Challenger* began positioning to the beacon in automatic mode. However, poor wind and sea conditions did not allow an immediate start at running the pipe in the hole. By 1118Z, the weather had moderated sufficiently for drilling operations to begin. Although the site had been originally scheduled for rotary drilling alone, a composite bottom hole assembly was made up to allow HPC after bit release. This was done to enable us to HPC the important Pleistocene section missed at Site 553 should it by chance be found during the rotary drilling. Hole 554 was spudded at 2017Z, 27 August, and a few pebbles set in mud indicated that the mudline had been just cut at 2584 m. Core 1 was cut from 2584.0 to 2593.5 m (Table 1) and continuous coring proceeded until 0712Z, 28 August, when yet another deterioration in weather conditions forced abandonment of the hole. The mudline was cleared at 0748Z, thereby completing Hole 554.

By 1203Z, 28 August, weather conditions had moderated enough for drilling to begin again and Hole 554A was spudded at 1248Z (Table 1). The interval 0–76 m subsea was washed. Core 1 cut between 76.0 and 85.5 m, and was followed by a heat-flow measurement (No. 8 of Leg 81). The hole was continuously cored to 114 m, where a second heat flow measurement (No. 9) was

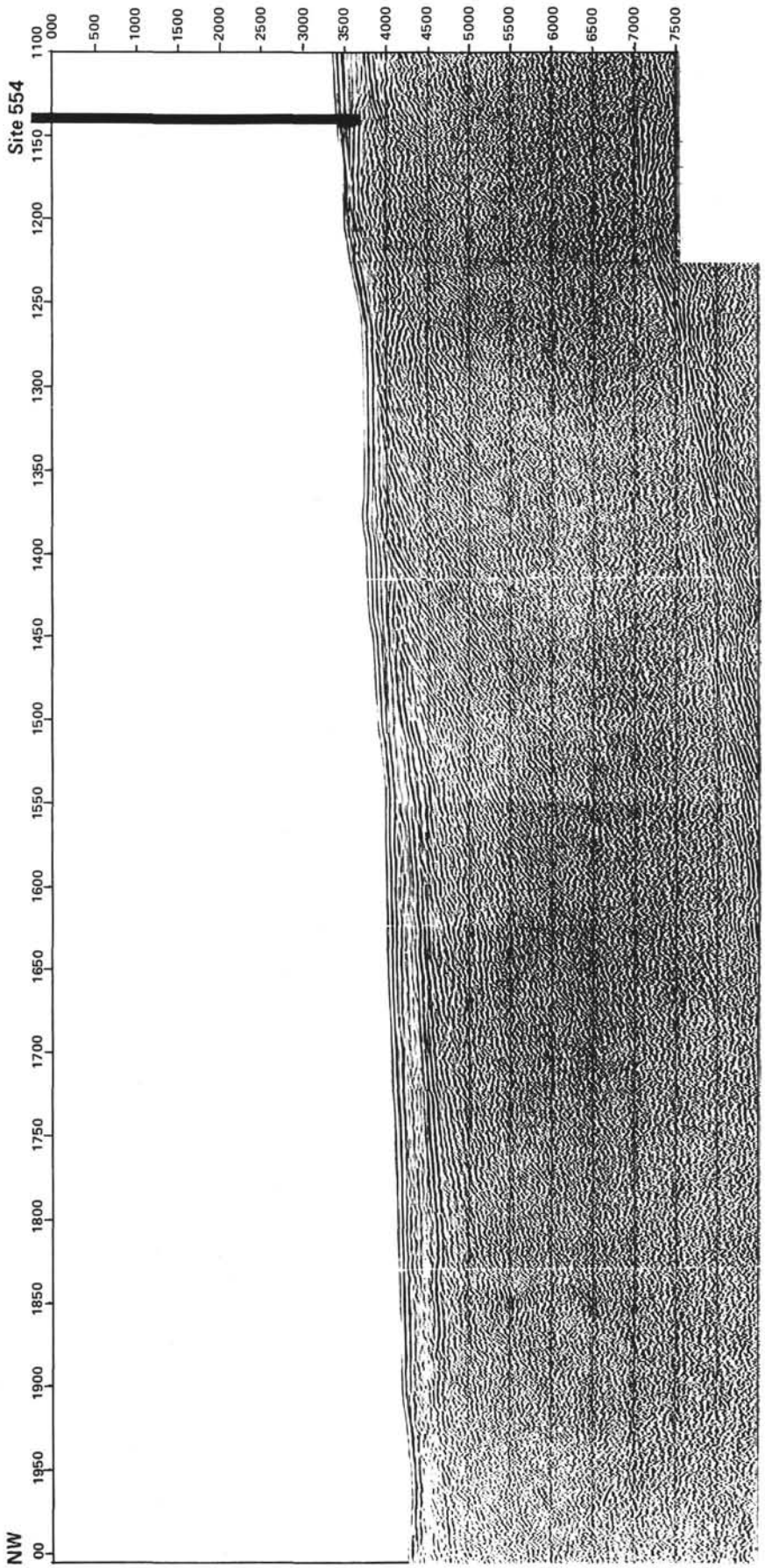
Site 554
NW
0
50
100
150
200
250
300
350
400
450
500
550
600
650
700
750
800
850
900
950
1000
1050
1100
1150
1200
1250
1300
1350
1400
1450
1500
1550
1600
1650
1700
1750
1800
1850
1900
1950
2000
2500
3000
3500
4000
4500
5000
5500
6000
6500
7000
7500

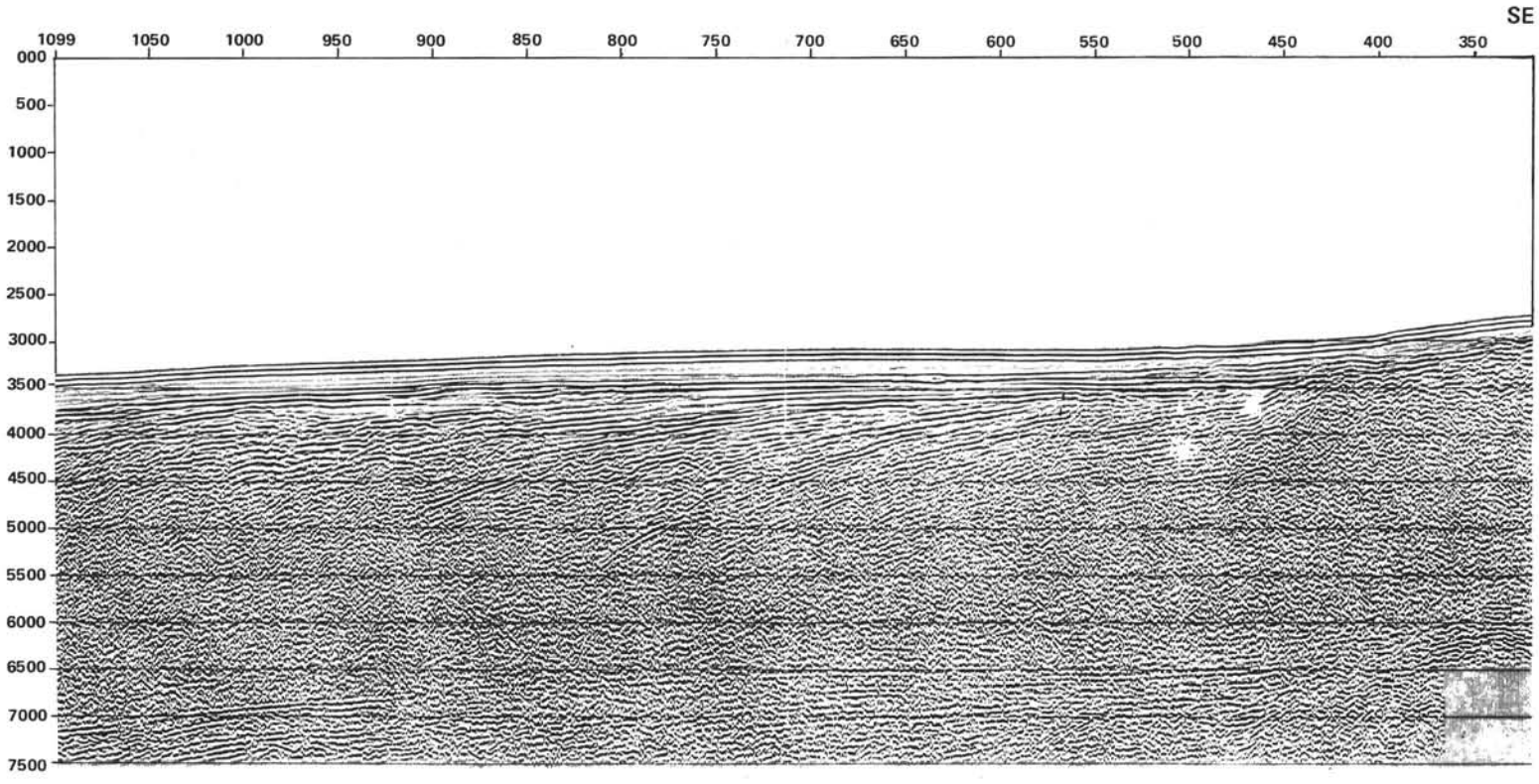

Figure 3. Multichannel seismic profile across the outer high (Line IFP-CEPM reproduced by kind permission).

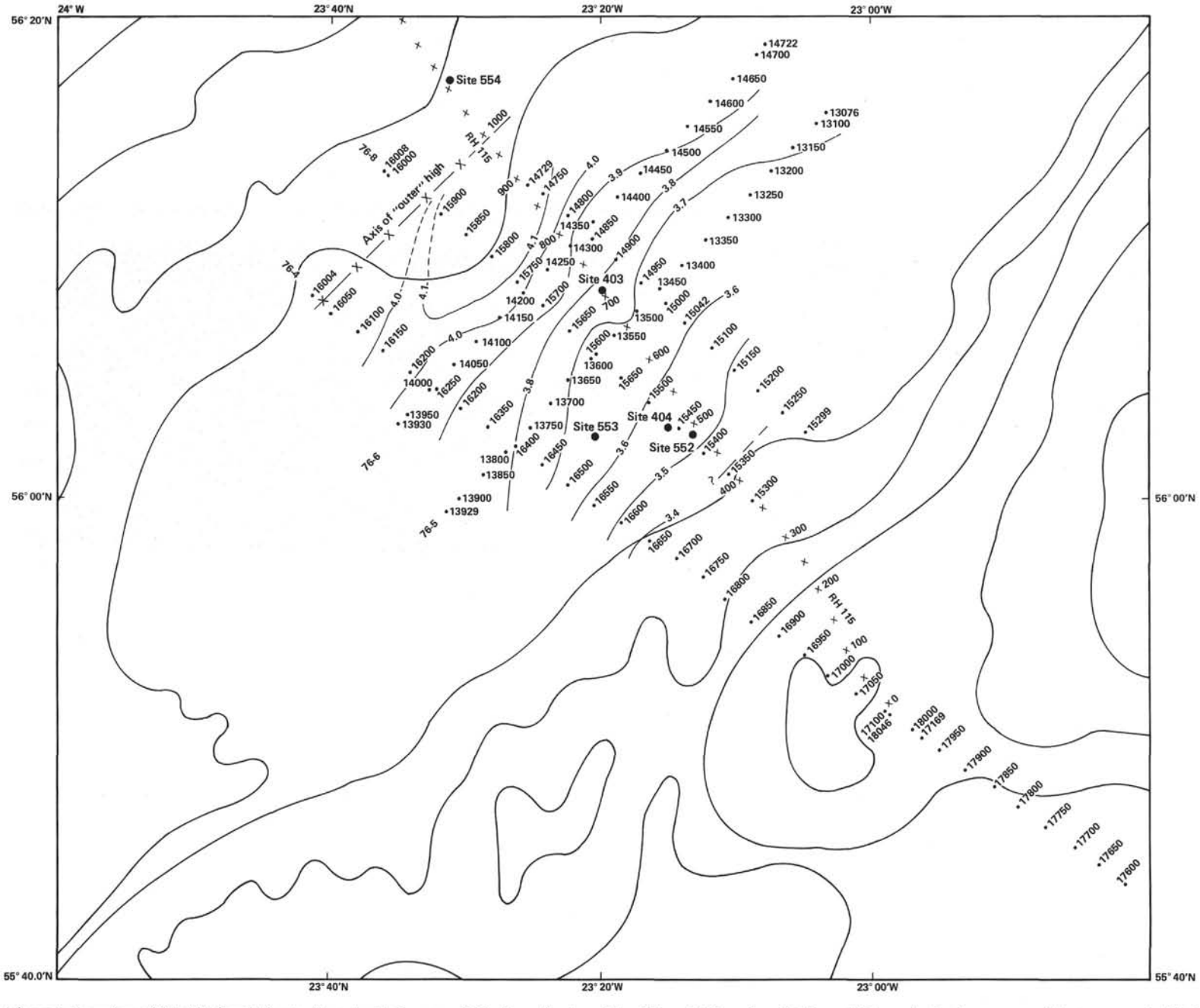

Figure 4. Location of Site 554 in relation to the outer high, zone of dipping reflectors, Sites 553 and 552, and available multichannel seismic coverage. (Contours marked 3.6 etc. are isochrons on top of dipping reflectors.)

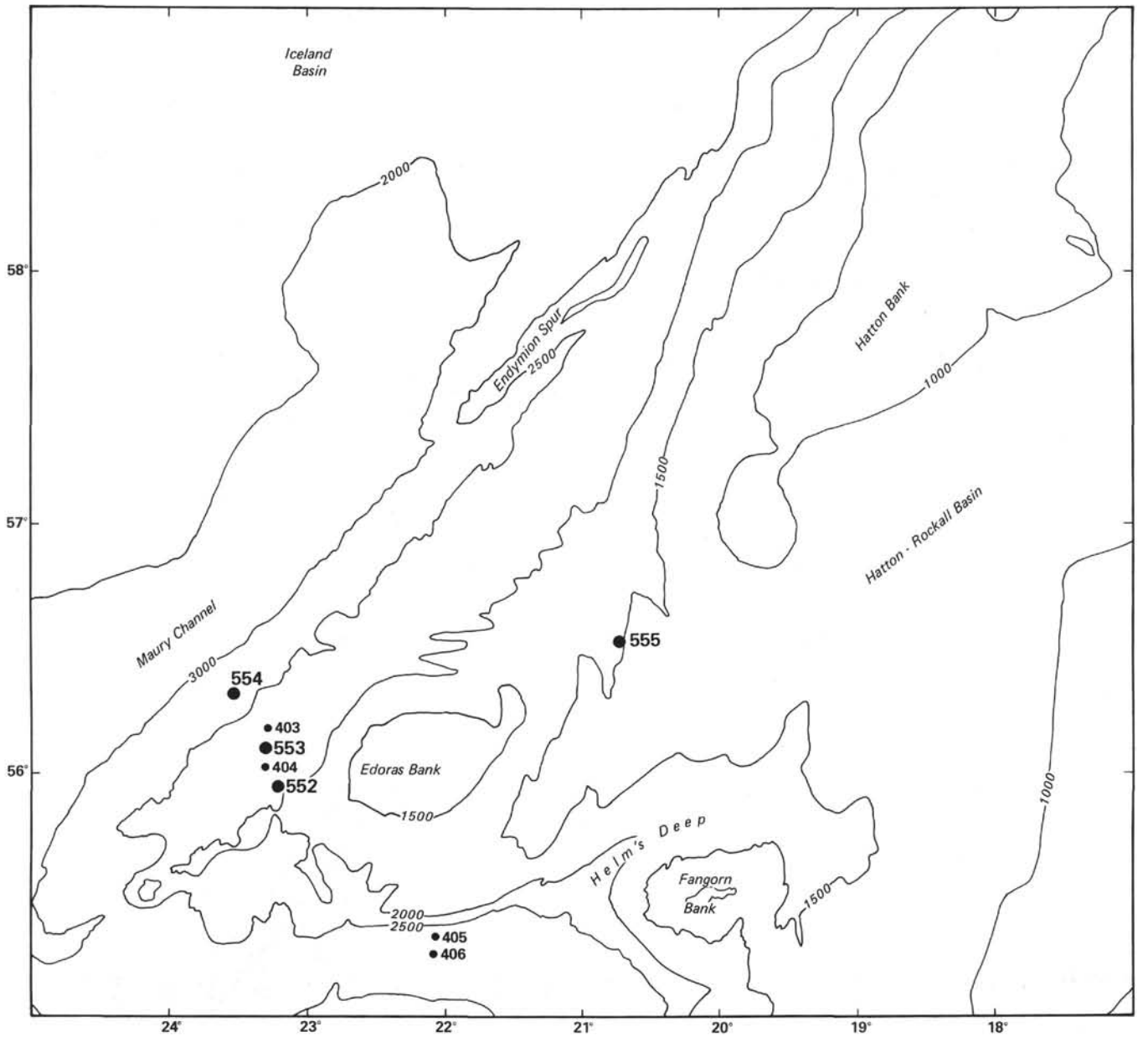

Figure 5. Bathymetry of Sites 552, 553, 554, and 555, Rockall Plateau.

made. At 2324Z, 28 August, the drilling rate slowed to 32 min./m in Eocene calcarenites overlying basalt. Cores 7 through 13 were cut with great difficulty in a sequence of basaltic lava flows and basaltic breccias. Continual sticking and torquing was experienced during cutting of the cores. Gel and guar was spotted between each core in an attempt to clear the hole, and several wiper runs were made. It was also necessary to pull back the pipe on two occasions to release it. Finally 145 barrels of mud were spotted after Core 13 but to no avail. In view of the continued difficult drilling conditions, Site 554 was abandoned at 1810Z, 29 August. The pipe was finally released from the hole at 1900Z after spotting a further 35 barrels of gel, and the bit reached the rig floor at 0051Z, 30 August. After securing the rig floor 0127Z, *Glomar Challenger* got underway, first steaming to the northwest until 0205Z to make a return crossing of Site 554. The beacon was crossed at 0257Z, 30 August, and at 0352Z, course was set 076° to make Site 555.

SEDIMENT LITHOLOGY

The 209 m section drilled at Site 554 can be divided into five principal lithologic units, four sedimentary units, and one interbedded volcanic and volcaniclastic unit. The lithologic divisions are summarized in Table 2 and Figure 7. A summary of the smear slide data is given in the appendix to this chapter.

Unit I: Core 554-1 to Sample 554-3,CC (0 to c. 28.5 m sub-bottom; 28.5 m thick). Age: Quaternary to late Pliocene.

This unit is characterized by alternating beds of white to light yellowish brown (10YR 8/2 to 10YR 7/3) foramin-

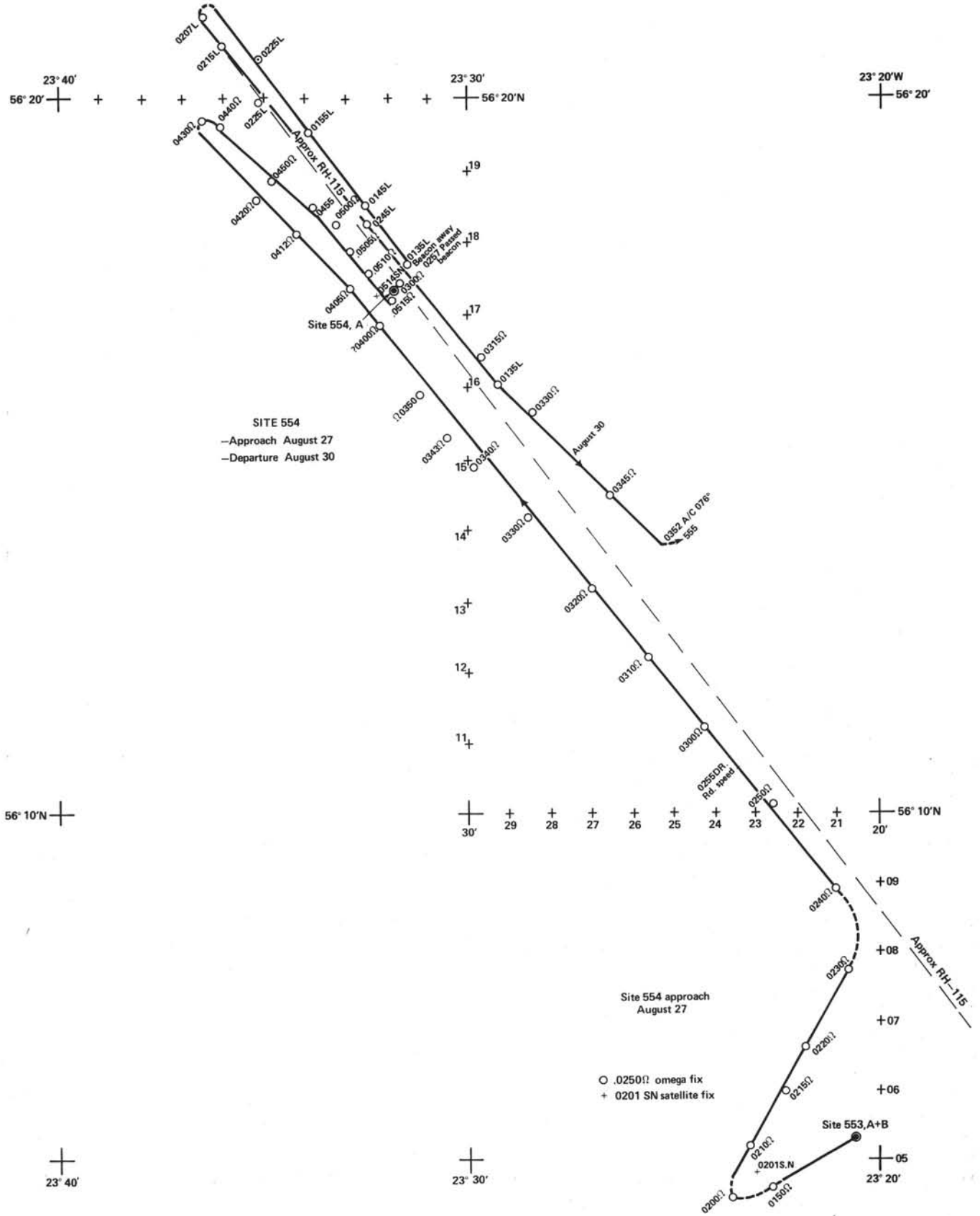

Figure 6. Approach of *Glomar Challenger* to Site 554.

Table 1. Coring summary, Holes 554 and 554A

Core	Date (Aug. 1981)	Time (Z)	Depth from drill floor (m) Top	bottom	Depth below seafloor (m) Top	bottom	Length cored (m)	Length recovered (m)	Percent recovered
Hole 554									
1	27	2221	2584.0-2593.5		0.0-9.5		9.5	6.26	66
2	27	2320	2593.5-2603.0		9.5-19.5		9.5	8.53	89
3	28	0030	2603.0-2612.5		19.0-28.5		9.5	8.98	94
4	28	0145	2612.5-2622.0		28.5-38.0		9.5	0.00	0
5	28	0256	2622.0-2681.5		38.0-47.5		9.5	9.30	98
6	28	0412	2631.5-2641.0		47.5-57.0		9.5	8.68	90
7	28	0525	2641.0-2650.5		57.0-66.5		9.5	5.97	63
8	28	0845	2650.5-2660.0		66.5-76.0		9.5	6.04	63
							76.0	53.76	71
Hole 554A									
1	28	1515	2660.0-2669.5		76.0-85.5		9.5	1.30	16
2	28	1740	2669.5-2679.0		85.5-95.0		9.5	2.97	34
3	28	1842	2679.0-2688.5		95.0-104.5		9.5	5.44	57
4	28	1948	2688.5-2698.0		104.5-114.0		9.5	5.01	54
5	28	2220	2698.0-2707.5		114.0-123.5		9.5	6.30	67
6	29	0005	2707.5-2717.0		123.5-133.0		9.5	3.47	37
7	29	0306	2717.0-2726.5		133.0-142.5		9.5	4.65	49
8	29	0503	2726.5-2736.0		142.5-152.0		9.5	2.92	32
9	29	0710	2736.0-2745.5		152.0-161.5		9.5	0.80	8
10	29	0933	2745.3-2755.0		161.5-171.0		9.5	0.56	6
11	29	1104	2755.0-2764.5		171.0-180.5		9.5	0.05	5
12	29	1235	2764.5-2774.0		180.5-190.0		9.5	0.15	2
13	29	1430	2774.0-2783.5		190.0-199.5		9.5	0.11	1
14	29	1810	2783.5-2793.0		199.5-209.0		9.5	0.80	8
							133.0	29.52	40

ifer or nannofossil-foraminiferal oozes and light brownish gray to light gray (2.5Y 6/2 to 2.5Y 7/2) foraminifer or nannofossil-foraminiferal muds. There is a minor amount of dark gray (2.5Y 4) sandy mud. Boundaries between the layers and the associated color change may be either gradational or sharp. These sediments are disturbed by drilling, and details of sedimentary structures, such as laminae, are not recognizable. Sand-size non-

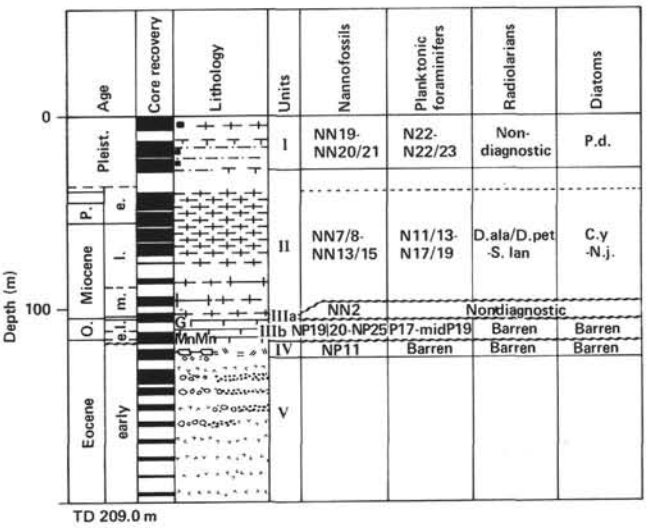

Figure 7. Lithologic and biostratigraphic summary, Holes 554 and 554A.

biogenic components (quartz, feldspars, heavy minerals, volcanic glass) are common in the muds and rare in the oozes. X-ray diffraction analysis of the fine fraction of the muds indicates the presence of smectite and illite in approximately equal proportions as well as about 10% chlorite.

The lower boundary of this unit is indeterminate and lies within Core 554-4 from which no sediments were recovered.

Unit II: Section 554-5-1 to Sample 8,CC; Core 554A-1 to Section 4-1 (c. 28.5 to 106.0 m sub-bottom;

Table 2. Lithologic units, Site 554.

Unit	Lithology	Sub-bottom depth (m)	Thickness (m)	Sedimentation rate (m/m.y.)	Age	Core-Section Hole 554	Core-Section Hole 554A
I	Foram ooze and minor foram-nanno ooze interbedded with foram mud and foram marl and minor nanno-foram mud and sandy mud. Terrigenous dropstones common.	0-28.50	28.50	17	Quaternary	1-1 to 3,CC	
II	Foram-nanno ooze with minor biosiliceous content, grading to chalk below 95 m.	28.50-106.00	77.50	7	early Pliocene to mid-Miocene	5-1 to 8,CC	1 to 4-1
IIIa	Glauconitic nanno-foram chalk.	106.00-106.25	0.25	<1	early Miocene		4-2 to 4-2, 25 cm
IIIb	Glauconitic foram chalk interbedded with biosiliceous foram marl and glauconitic foram marl. Manganese layer at base.	106.25-118.80	12.55	<1	Oligocene to late Eocene		4-2, 25 cm to 5-4, 30 cm
IV	Zeolitic tuffaceous marlstone, zeolitic calcareous tuff and zeolitic tuff. Lapilli are common.	118.80-126.60	7.80	<1	early Eocene		5-4, 30 cm to 6-3, 10 cm
V	Volcanogenic conglomerates and volcanogenic sandstones interstratified with basalt lava flows.	126.60-209.00	82.40		Probably early Eocene		6-3, 10 cm to 14

about 77.50 m thick). Age: early Pliocene-middle Miocene.

This unit consists of uniform bluish white (5B 9/1) foraminifer-nannofossil or nannofossil-foraminiferal oozes which grade to chalk below 95 m. Fine laminations are abundant, with color ranging from very light gray (N8) and light bluish gray (5B 7/1) to pale olive (5Y 6/3) without noticeable compositional or textural variations. Bioturbation is minor throughout. The coarse fraction contains rare benthic foraminifers and biogenic siliceous components. The nonbiogenic fine fraction consists predominantly of smectite and mixed-layer minerals. Sand-size terrigenous particles are absent.

The first appearance of nannofossil-foraminiferal chalk occurs at 95 m. Below this depth, chalk layers (about 10 cm) are interbedded with foraminifer-nannofossil oozes. The boundary between these layers is gradational. At 99 m the color of the foraminifer-nannofossil ooze changes from bluish-white to white (N9) with faint color cycle from white to gray (5Y 6/1).

Unit III: Core 554A-4 to Sample 5-4, 30 cm (106.0 to 118.80 m sub-bottom; 12.80 m thick). Age: early Miocene, late and early Oligocene to late Eocene.

Subunit IIIa: (106.0 to 106.25 m). Age: early Miocene.

This unit is characterized by pale yellow (2.5Y 8/4) to olive gray (5Y 5/2) glauconitic nannofossil-foraminiferal or foraminifer chalks. The top of this unit is marked by a hiatus below the middle Miocene; a marked hiatus also occurs at the lower boundary of the subunit.

Subunit IIIb: (106.25 to 118.80 m). Age: Oligocene to late Eocene).

This subunit is characterized by yellow (2.5Y 8/6) glauconitic nannofossil-foraminiferal or foraminifer chalks interbedded with grayish-brown (2.5Y 5/2) to olive brown (2.5Y 4/4) glauconitic or biosiliceous foraminiferal marls. The latter interbeds contain a minor but persistent component of biogenic silica (radiolarians, sponge spicules) and fish teeth. The bioturbation is moderate, and the contacts between the lithologies are sharp. Both planar and cross-lamination as well as microfaults are common in this subunit.

Glauconite content increases toward the bottom of this subunit and is often concentrated within laminae; the abundance of foraminiferal marl layers, however, decreases toward the bottom.

The base of the subunit is marked by a manganese layer, 10 cm in thickness, which overlies shallow marine sediments of early Eocene age. Dispersed in a matrix of foraminiferal chalk, the manganese layer includes: massive Mn-rich micronodules, Fe-Mn microconcretions, and micronodules of Fe-rich smectites showing botryoidal texture. Also present are basaltic fragments with hematite crusts, primary detrital minerals (magnetite, pyroxene, and plagioclase feldspar), as well as secondary authigenic products such as glauconite replacing foram tests and phillipsite and barite in the core of smectite and Mn-rich concretions.

Unit IV: Samples 554A-5-4, 30 cm to 6-3, 10 cm (118.80 to 126.60 m sub-bottom; 7.80 m thick). Age: early Eocene.

The top of this unit is an unconformity below the manganese layer; the base is defined by a change to conglomerate. The unit consists of yellowish brown (2.5YR 5/4) to dark brown (10YR 3/3) zeolitic tuffaceous marlstone, zeolitic calcareous tuff, and zeolitic tuff. Green lapilli, angular and rounded, and sand-size dark brown and light olive altered palagonitized glass fragments are included in a matrix of clay and zeolite or cemented by well-crystallized calcite (sparite). X-ray diffraction (XRD) analyses show that the clay consists only of Fe-smectites, poorly or moderately crystallized, and that the zeolite is phillipsite. This assemblage could result from the *in situ* devitrification of volcanic glass. The biogenic components are mainly foraminifers and scattered fragments of shells which occur throughout this unit. Burrows are common, but the bioturbation is minor and is insufficient to destroy the laminations. There is some cross-laminated sediment.

Unit V: Samples 554A-6-3, 10 cm to 14-1, 100 cm (126.0 m sub-bottom to total depth of hole at 209 m; 82.60 m thick). Age: not established (probably early Eocene).

This unit consists of volcanogenic conglomerates and sandstones interstratified with basalt lava flows (Tables 2, 3). The top of the unit is marked by a 15-cm-thick granule to small pebble-size conglomerate. This conglomerate contains rounded and small angular clasts of basalt, highly altered basalt, and palagonite. The clasts are yellowish brown (10YR 5/4) to dark yellowish brown (10Y 4/4), and they are cemented by white (10YR 8/2) calcite spar. Some of this cement may be recrystallized calcareous sediment from the marl above, which filtered into the gravel soon after deposition. There is no clay matrix nor is there any other terrigenous detritus. The contact with the underlying altered basalt (pale brown, 10YR 6/3) is sharp, and the basalt lacks a palagonite or glassy margin. This suggests that the contact is erosional, and the conglomerate could represent a transgressive pebble beach or very shallow marine sediment deposited

Table 3. Interrelation of basalts and sediments.

Core	Interval recovered (m sub-bottom)	Lithology
6	126.6–126.75	Conglomerate
	126.75–127.0	Basalt
7	133.0–138.15	Basalt
	128.15–139.25	Conglomerate
	139.25–139.48	Basalt
8	142.5–143.25	Conglomerate + sandstone
	143.25–144.15	Basalt
	144.15–145.9	Conglomerate + sandstone
9	152.0–152.75	Conglomerate
	152.75–153.15	Basalt
10	161.5–161.6	Conglomerate
	161.6–162.2	Basalt
11	171.0–171.1	Basalt
12	180.5–180.65	Basalt
13	190.0–190.1	Basalt
14	199.5–200.5	Basalt

under high-energy conditions such as those generated by wave action.

The recovery rate of only 16% makes it impossible to determine the exact proportions of sediment and basalt. At least four conglomerate and sandstone interbeds occur (in Cores 7, 8, 9, and 10) between basalt flows. Cores 11 to 14 contained only basalt, although (because of the poor recovery) sediments may be present in this interval.

A total thickness of approximately 4 m of sediment (conglomerate plus sandstone) was recovered. The thickest sediment interbed was 1.75 m in the base of Core 8 and consisted of a well-sorted volcaniclastic sandstone overlying a matrix (sand) supported conglomerate and a clast supported conglomerate, with all lithologies cemented by sparry calcite.

Characteristic features of the sandstones and conglomerates are (1) the lack of mud, (2) the uniform basaltic composition of clasts, (3) the lack of any sedimentary structures such as bedding, and (4) the lack of bioclastic carbonate. Thus the sediment is totally derived from the breakup of submarine basalt flows. Some sand has penetrated down fractures in the underlying basalt, and some basalt boulders, of at least 25 cm diameter, are present in the sandstone. The sand clasts are generally coarse, well-sorted, and subrounded. Geopetal features in Section 7-4 are formed by sand filtering down into the underlying clast supported conglomerate and leaving cavities later filled by calcite spar (Fig. 8). The clasts in the conglomerates are angular to subrounded, and the pebble size is bimodal (0.5 to 1 cm and 2 to 5 cm). The irregular shape of some pebbles results from fracturing through vesicles. The pebbles are composed of either basalt or palagonite, with some basalt pebbles having a palagonite rind on part of their surface indicating that they were mechanically broken after formation of the palagonite.

The sediment in this unit has characteristics that suggest an environment of deposition just below wave base, perhaps near a relatively high-energy shoreline.

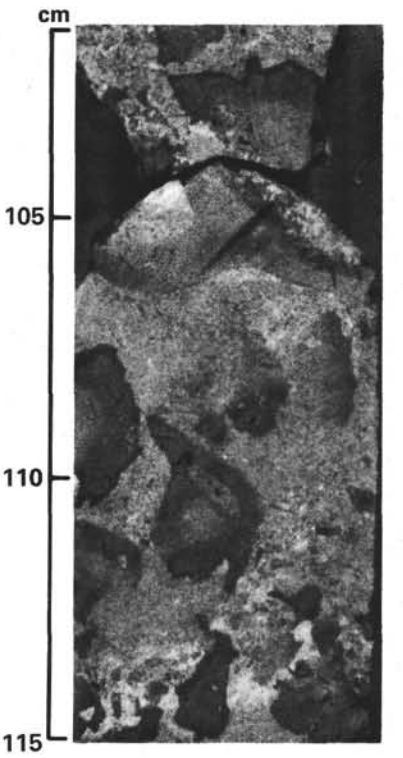

Figure 8. Geopetal structure (Sample 554A-7-4, 102–115 cm).

BIOSTRATIGRAPHY

Site 554 was drilled at a water depth of 2574 m on the "outer high" of the southwest margin of the Rockall Plateau. A total of 14 sedimentary cores were recovered, 8 from Hole 554, and 6 from Hole 554A. The uppermost 106 m represents the Neogene, and the interval between 106 m and the sediment/basalt contact at 126.5 m is Oligocene and Eocene in age. Two major unconformities occur. The first is between the middle Miocene and the early Miocene and the second between the late Eocene and the early Eocene.

Benthic foraminifers indicate that deposition took place at depths very similar to the present site depth from the middle Miocene to the present. A progressive deepening is recorded from the early Eocene (75–125 m) to the early Miocene (deeper than 1900 m).

Calcareous microfossils are abundant and comparatively well-preserved in the Holocene–upper Eocene interval. Nannofossils are rare and generally poorly preserved in the lower Eocene sequence. Siliceous microfossils are not preserved in the middle and lower Pleistocene, in a short interval in the upper Miocene, and in the lower Eocene.

It should be noted that the first occurrence of *Globorotalia truncatulinoides* is missing in the sedimentation rate plot for Site 554. This taxon is present in Sample 554-1,CC but is absent in 2,CC and 3,CC. According to results obtained from Sites 552 and 553, *G. truncatulinoides* has a regional first occurrence at between approximately 0.9 and 1.1 m.y. ago in this part of the Atlantic Ocean. However, the planktonic foraminiferal assemblage in Sample 544-2,CC is dominated by *Neogloboquadrina pachyderma*, the mass occurrence of which indicate cool surface-water temperatures. In consequence, *G. truncatulinoides* may have been temporarily excluded from the foraminiferal assemblage in Sample 554-2,CC for paleoecological reasons. It follows that the first occurrence level of *G. truncatulinoides*, even within a small geographic area, has to be considered with great care before being adopted as a biostratigraphic marker.

A discrepancy occurs between the diatom biostratigraphy and other microfossil groups for the interval from Samples 554-7-3, 80–82 cm to 554A-1-1, 5–17 cm. The first occurrence of *Thalassiosira miocenica* and *T. convexa* s. ampl. occurs in the interval between Samples 554-8,CC and 554A-1-1. According to Burckle and Trainer (1979), the first occurrences of these taxa occur in Epoch 6, which gives an age of approximately 6.2 m.y. ago for these datum events. *T. praeconvexa* has a short range between approximately 5.8 and 6.4 m.y. ago. This species thus overlaps the first occurrences of *T. miocenica* and *T. convexa* s. ampl. In Site 554 *T. praeconvexa* is present from 554-8,CC (not present in 7,CC) to 554A-

1-1, 15–17 cm. According to diatom biostratigraphy, the transitional interval between 554-8,CC and 554A-1-1 suggests an age close to 6 m.y. ago. However, nannofossils and radiolarians suggest an age of approximately 6 m.y. ago in the upper part of Core 554-7 and 6,CC. The cause for this age–depth discrepancy is not fully understood (see Baldauf, this volume, for further discussion of this problem).

The condensed Oligocene–late Eocene sequence, in which 15 m.y. are represented in 12.5 m of sediments, is remarkable in the sense that at least a part of all the nannofossil zones between NP25 and NP19/20 are apparently present. In spite of the condensed nature of this sequence, it is thicker than any other Oligocene–late Eocene interval recovered during Leg 81. Furthermore, there is a trend of increasing thickness of the recovered Oligocene sediments from east to west through Sites 552, 553, and 554, although only the upper part of the Oligocene (NP24/NP25) is present at Site 553. The youngest 8.5 m.y. of the Oligocene (NP23–NP25) represent a period of low biostratigraphic resolution in the nannofossil record in the high latitude North Atlantic Ocean. This results first from the great length of Zone NP23 (5.5 m.y.), and second from the virtual absence of the sphenolith taxa which define the NP23/NP24 and NP24/NP25 boundaries. From her studies of the North Atlantic Ocean, Müller (1979) suggested that the first occurrence of *Triquetrorhabdulus carinatus* and *Cyclicargolithus abisectus* approximates the NP24/NP25 and NP23/NP24 boundaries, respectively. These events have been used to determine these zonal boundaries at Site 554. However, the condensed character of the Oligocene sequence and the relatively rare occurrences of *T. carinatus* in that sequence are bound to provide a less precise determination of the NP24/NP25 boundary. Forms intermediate between *C. abisectus* and *C. floridanus* occur in the lowermost part of the range of the former species. A biometric study—for example, of diameter size—aimed at evaluating the taxonomic relationship of these two taxa probably would enhance a greater consistency between workers using the first occurrence of *C. abisectus* as an auxiliary marker fossil.

The unconformity separating the late and early Eocene occurs at Sample 5-4, 31 cm. An 11-cm-thick layer of manganese nodules is present at the contact. The early Eocene sequence is intensively burrowed. Late Eocene nannofossils are present in burrows to a depth of 35 to 40 cm below the manganese layer.

Calcareous Nannofossils

Hole 554

Sample 554-1,CC is of late Pleistocene age (Zones NN20/NN21), showing a nannofossil assemblage identical to those observed at Sites 552 and 553. *Pseudoemiliania lacunosa* was observed in Sample 554-2-2, 85 cm, indicating Zone NN19. *Calcidiscus macintyrei* has its last occurrence between Samples 554-3-4, 50 cm and 3-5, 35 cm. Discoasters are not present in 3,CC, implying that this sample belongs to the lower part of Zone NN19. Core 4 had no recovery. The top of Sample 554-5-1, 70 cm, contains the following marker fossils; *Ceratolithus rugosus, Discoaster brouweri, D. pentaradiatus, D. surculus, Reticulofenestra pseudoumbilica*, and *Sphenolithus abies*. This association suggests that this sample may range from Zones NN13 to NN15. *Amaurolithus delicatus* was observed at Sample 554-5-6, 140 cm together with the aforementioned species (except *C. rugosus*). Since *A. delicatus* is closely related to *A. tricorniculatus* whose extinction defines the NN14/NN15 boundary, it follows that this sample may be assigned to a zone older than NN15, but the assemblage in this sample does not allow a precise determination of its oldest possible age.

The NN11/NN12 boundary occurs between Samples 554-6-5, 46 cm and 6,CC. *A. delicatus* was observed in 7,CC together with *D. quinqueramus*, suggesting that this sample should be referred to the later part of Zone NN11. Sample 8,CC also represents Zone NN11.

Hole 554A

A sample from the core catcher of Core 554A-1 shows a fairly diverse assemblage, including *Discoaster quinqueramus, D. loeblichii, D. prepentaradiatus*, and *D.* sp. cf. *D. neorectus*. The morphology of the last species matches well with the description of *D. neorectus* Bukry. However, the largest specimen observed in 1,CC is only 18 μm, which is somewhat below the size range indicated by Bukry. Nevertheless, the discoaster association indicates that this sample belongs to the *Discoaster neorectus* subzone of Bukry (1973), which correlates with the lowermost part of Zone NN11. Of the above listed discoasters only *D. prepentaradiatus* was observed in 2,CC. Hence, this sample probably belongs to Zone NN9 or NN10.

Abundant large *Dictyococcites perplexus* dominate the assemblage at Sample 554A-3-3, 90 cm. Rare specimens of *Discoaster calcaris* and *D. brouweri* were also observed, indicating that this sample probably belongs to Zone NN9. A sample at 3-3, 145 cm contains *Coccolithus miopelagicus, D. exilis, Sphenolithus abies*, and large *Reticulofenestra pseudoumbilica*. This association is present throughout Section 554A-4-1. Since *Cyclicargolithus abisectus, C. floridanus*, or *Sphenolithus heteromorphus* were not observed in that sequence it is referred to Zones NN7/NN8. An early Miocene sequence was observed at Sample 4-2, 21 cm. The nannofossil assemblage includes *S. belemnos* and *Triquetrorhabdulus carinatus*, suggesting that the sample probably represents Zone NN2.

Zone NP25 of the late Oligocene is present from Sample 554A-4-2, 35 cm and throughout the section. The assignment is based on the presence of *Dictyococcites bisectus* and *T. carinatus*. Two specimens of *S. ciperoensis* were observed at 80 cm in this section. A condensed sequence of late Oligocene age is present throughout the remaining part of Core 4. The zonal boundaries of the late Oligocene, NP24/NP25 and NP23/NP24, are difficult to identify at high latitudes because marker fossils are lacking or are extremely rare. However, Zone NP24 is probably represented at Sample 554A-4-3, 80 cm since *Cyclicargolithus absectus* is a common member of the

assemblage at that level. *Chiasmolithus oamaruensis* was observed at Sample 554A-4-3, 145 cm, whereas *C. abisectus* is very rare at that level. This may indicate that the 145-cm level represents Zone NP23. The first downhole occurrence of *Isthmolithus recurvus* was observed at Sample 554A-4-4, 25 cm.

Common *Chiasmolithus altus*, few *C. oamaruensis, R. umbilica*, and *I. recurvus* occur in 4,CC, suggesting Zone NP22 of the early Oligocene. At Sample 554A-5-1, 58 cm *R. umbilica* and *I. recurvus* are both common, but *Calcidiscus formosus* was not observed here, indicating Zone NP22.

The first downhole occurrence of *C. formosus* was observed in Sample 554A-5-3, 48 cm, indicating the NP21/NP22 boundary at that level. At 554A-5-3, 104 cm Eocene discoasters (*D. barbadiensis* and *D. saipanensis*, the extinctions of which define the NP19–20/NP21 boundary), and *Reticulofenestra reticulata* were observed, together with common *R. umbilica, D. bisectus, I. recurvus*, and abundant *Ericsonia fenestrata*. This association occurs down to the 20 cm level in Section 554A-5-4, where a 11-cm-thick manganese layer abruptly marks the lower boundary of the overlying sequence of calcareous ooze.

An intensively burrowed, lithified zeolitic mudstone is present below the manganese layer in Core 5. This unit is fossiliferous down to 5,CC. Thirteen samples have been investigated from Sample 554A-5-4, 34 cm to the bottom of Core 5. The rarely occurring nannofossil assemblages are virtually identical in composition, with *Toweius occultatus, Calcidiscus formosus,* and *C. Pelagicus* as the most common taxa. The following species were also observed: "*Coccolithus*" *luminis, Chiasmolithus solitus, Discoaster binodosus, D. diastypus, D. keupperi, D. multiradiatus, D. robustus, Markalius astroporus, Neococcolithes dubius, Pontosphaera fimbriata, P. pulchra, P. rimosa, P. versa, Prinsius bisulcus, Toweius* cf. *magnicrassus*, and *Tribrachiatus orthostylus*. The presence of *T. orthostylus* and the absence of *D. lodoensis* from Sample 554A-5-4, 50–92 cm suggests that this part of Core 5 belongs to Zone NP11. *Ellipsolithus macellus* and *Chiasmolithus bidens* are present in 5,CC, possibly indicating Zone NP10. At Sites 552, 553, and 555 these two taxa disappear shortly before the first appearance of *Tribrachiatus orthostylus*, which is used to define the NP10/11 boundary.

Core 6 is barren of identifiable nannofossils.

Planktonic Foraminifers

Hole 554

Sample 554-2,CC is probably of late Pleistocene age based on the occurrence of *Globorotalia truncatulinoides* which makes its first local appearance in this area in the middle part of the Pleistocene. Samples 2,CC and 3,CC are probably from the middle to early Pleistocene. *G. inflata* and *Neogloboquadrina pachyderma* s.s. are abundant but *G. truncatulinoides* does not appear in these two samples. However, Sample 2,CC is characterized by a dominance of *N. pachyderma* which suggests more severe climatic conditions. Thus it is possible that *G. truncatulinoides* may occur below 2,CC in sediments deposited during less severe, interglacial conditions. There was no recovery in Core 4.

Sample 554-5,CC is of earliest Pliocene or latest Miocene age based on the stratigraphic position and the occurrence of *G. margaritae* and *G. conoidea* in the absence of *G. puncticulata*. Sample 6,CC is characterized by very low diversity and by very high faunal dominance by *Neogloboquadrina atlantica* and its related forms *G. acostaensis* and *N. pachyderma*. No specific age can be placed on the sample other than early Pliocene–late Miocene (N19–N17). Samples 7,CC and 8,CC are late Miocene (N17 or N16) in age based on the concurrence of *G. margaritae* and *G. miotumida* and by the presence of *Globigerina praebulloides*.

Hole 554A

Sample 554A-1,CC is dominated by *Globorotalia conoidea, Globigerina praebulloides*, and *Neogloboquadrina pachyderma* s.l, whereas *Globorotalia miotumida* is common and *Globigerina woodi* is rare. In this area, this association can occur from N15 through N17. However, the dominance of the assemblage by *G. conoidea* appears in this area to be associated with the coiling change of *N. atlantica* and the coiling change does occur between Samples 1,CC and 2,CC. The coiling change also corresponds approximately to the NN10/NN11 boundary of the calcareous nannofossils in Hole 552A. This correlates with the middle of N16. Therefore it is suggested that Sample 1,CC is approximately in the middle of N16. Little is present in Sample 2,CC to indicate a precise age. The presence of *Globorotalia menardii, Globigerina woodi, G. praebulloides*, abundant *N. atlantica*, and frequent *N. pachyderma* s.l. indicate a late Miocene age that may be either N16 or N15.

Sample 554A-3,CC is probably referable to Zone N14 based on the occurrence of *Globorotalia mayeri, G. acrostoma*, and *G. miozea miozea*, and *G. miozea panda*. It is to be noted that *G. acostaensis, Neogloboquadrina atlantica, N.* cf. *humerosa, N.* cf. *eggeri*, and *N. pachyderma* are abundant in this sample (as parts of the *Neogloboquadrina* plexus). There is no indication of reworking. Therefore a late middle Miocene age is suggested for the sample.

Sample 4,CC is early Oligocene in age based on the occurrence of *Globigerina angiporoides*.

Radiolarians

Cores 554-1 through 8 and 554A-1 through 4 (115 m) contain radiolarians of Quaternary through Oligocene age.

Three barren intervals correlate to barren intervals of the same ages at Sites 553 and 552: part of the Pleistocene and upper Pliocene (554-2,CC through 3-5), part of the upper Miocene *Didymocyrtis penultima* through *D. antepenultima* Zones (554A-1,CC through 2,CC), and the early Eocene of Cores 554A-5 through 6. At all three sites, radiolarians are present, but diluted greatly in the top 10 to 15 m of Pleistocene sediments; then for the next 10 to 15 m they are completely missing. It is difficult to say whether this is an effect of masking by terrig-

enous components or a combination of masking and dissolution. In preglacial sediments siliceous fossils are few to common and well preserved. The barren intervals in the Miocene are obviously a result of diagenesis since preservation declines above and below the interval, and the barren preparations sometimes contain fragments and clay flocules encasing partly dissolved specimens. Because this barren interval is controlled by time rather than depth, it can be assumed that the dissolution took place near the time of deposition. And since the rate of carbonate deposition throughout the late Miocene and early Pliocene is steady, indicating a uniform depositional environment, an explanation for increased dissolution at this time segment may be that the amount of silica originally deposited is small. The absence of siliceous fossils in the early Eocene sediments may also be a dissolution effect: It is possible that the early Eocene shallow water at these sites was silica-poor or highly alkaline and therefore unfavorable for preservation of siliceous skeletons.

Age Assignments

Samples 554-1,CC through 2-3, 12–14 cm are considered younger than 425,000 years old because they appear to be above the extinction of *Stylatractus universus*. Samples from 554-2,CC through 4,CC are barren. Core 554-5 is assigned to the *Sphaeropyle langii* Zone (Foreman, 1975) on the co-occurrence of *S. langii* and *Stichocorys peregrina*. Samples 554-8,CC and 554A-1-1, 18–20 cm are apparently very near the evolutionary transition between *S. delmontensis* and *S. peregrina* and therefore near the boundary between the *S. peregrina* and *D. pentultima* Zones. The radiolarian assemblage in Sample 554A-1,CC is largely dissolved and samples from Core 554A-2 and Core 3, Section 1 contain only fragments and rare sponge spicules. Below Section 554A-3-3, radiolarians are rare and poorly preserved, but the presence of *Didymocyrtis laticonus* and *Cyrtocapsella japonica* suggest a middle Miocene age, equivalent to the *Diartus petterssoni* or *Dorcadospyris alata* Zones (Riedel and Sanfilippo, 1978). These species and the common occurrence of *C. tetrapera* with rare *Lithopera renzae* place Sample 554A-4-2, 2–4 cm in the *D. alata* Zone. The absence of *C. tetrapera* in an assemblage similar to that in the previous hole (Sections 553A-8-4 through 9-3) places Sample 554A-4-3, 18–20 cm below the early Miocene *C. tetrapera* Zone. Samples below 554A-4,CC are barren of radiolarians.

Diatoms

Hole 554

Samples examined from Site 554 contain few to common diatoms. Preservation varies between samples but is generally poor. A late Quaternary age is given to Core 554-1 based on the occurrence of *Pseudoeunotia doliolus* and *Rhizosolenia curviostris*.

With the exception of Sample 554-5,CC, the interval from Cores 2 through 6 represents a dissolution interval containing rare diatoms. Sample 554-5,CC contains few well-preserved diatoms. This sample is placed in the *Nitzschia jouseae* Zone based on the rare occurrence of *N. jouseae*. Other species present include *Thalassiosira oestrupii, Nitzschia fossilis, Coscinodiscus nodulifer, Nitzschia reinholdii*, and *Rhizosolenia barboi*.

Cores 7 and 8 are placed in the late Miocene portion of the *Thalassiosira convexa* Zone based on the presence of *Thalassiosira miocenica, T. nativa*, and *Nitzschia cylindrica* without *T. oestrupii*.

Hole 554A

Core 554A-1 through Core 3, Section 3 are placed in Subzone b of the *Nitzschia miocenica* Zone of Burckle (1972, 1977). This age assignment is based on the occurrence of *Thalassiosira praeconvexa* and *Nitzschia cylindrica* without the presence of *T. miocenica* and *T. convexa* s. ampl. The common occurrence of *T. eccentrica* and the *Nitzschia marina-reinholdii* group support this age assignment.

Section 554A-3-4 is tentatively placed in the *Coscinodiscus yabei* Zone. This age assignment is based on the presence of *Nitzschia cylindrica, Hemidiscus cuneiformis*, and *Thalassiosira* sp. 1., and the absence of the *N. marina-reinholdii* group.

Benthic Foraminifers

All the Neogene assemblages are similar, with *Planulina wuellerstorfi, Oridorsalis umbonatus*, and *Epistominella exigua* being present in almost every sample. The glacial part of the succession contains *Triloculina frigida, Cassidulina teretis*, and *Pyrgo bulloides*—not seen in the preglacial succession. However, the latter includes several species not found in the glacial succession, namely *Cibicidoides kullenbergi, Bulimina alazanensis, Globocassidulina subglobosa, Brizalina subaenariensis, Ehrenbergina serrata, Laticarinina pauperata*, and *Bulimina striata*.

Diversity is generally high ($\propto$12 to 20), and there is an overall trend of diversity increase from the mid-Miocene ($\propto$12 to 13) to the Pleistocene ($\propto$16 to 20).

The planktonic:benthic ratio is 99:1 and indicates open ocean conditions. The presence of the *Planulina wuellerstorfi* fauna throughout the Neogene indicates the existence of North Atlantic Deep Water and depths more than 1500 m. *Melonis pompilioides* occurs in low abundance and may indicate depths more than 2000 m. *Sigmoilopsis schlumbergeri* is generally rare, suggesting depths greater than 2200 m. *Epistominella exigua* commonly forms 5 to 10% of the assemblage and in Sample 554-2,CC it reaches 12.5%. Values greater than 20% are characteristic of depths greater than 2900 m. From these observations, it may be concluded that the water depth throughout the Neogene was in the range from 2200 to 2900 m.

The Oligocene and late Eocene assemblages (Samples 554A-4-2, 47 cm and 5-4, 12 cm) have a high planktonic:benthic ratio and generally moderate diversity (total range $\propto$6 to 20). The dominant forms are *Nodosaria-Stilostomella* spp., *Gyroidinoides* spp., and *Oridorsalis ecuadorensis* . In the late Oligocene other common forms include *Spiroplectammina spectabilis* and *Melonis* spp., while in the early Oligocene these species occur in low

abundance. This suggests a water depth greater than 700 m. There is a possibility that some dissolution may have taken place in these assemblages.

The early Eocene of Sample 554A-5,CC is a hard zeolitic marlstone. This was crushed under water in a mortar and then sieved. The foraminifers recovered are in remarkably good condition and include *Bolivinopsis adamsi, Lenticulina* spp., *Anomalinoides howelli, A. nobilis*, and *Pulsiphonina prima*. Sample 554A-6-1, 118 cm has a planktonic:benthic ratio of 55:45 and a benthic diversity of ∝19. The dominant forms are *Anomalinoides howelli, Gyroidinoides* spp., *Globocassidulina subglobosa*, and *Eponides* spp. These samples represent shelf conditions of mid- to outer-shelf depths (100–150 m). The lowest sample, 554A-6-3, 3–4 cm, from above the basalt, yielded a sparse fauna of *Alabamina obtusa, Anomalinoides howelli*, and *Pararotalia lecalvezae*. This suggests midshelf depths of 75–150 m.

Thus, this site records subsidence from midshelf in the early Eocene to epibathyal in the Oligocene and lower mesobathyal in the Neogene.

SEDIMENT ACCUMULATION RATES

The sedimentary thickness of 130 m at Site 554 represents approximately 52 m.y. The sediments at Sites 552 and 553 cover a comparable time span, but the thickness is much greater at these sites. This difference between Sites 552 and 553 on the one hand and Site 554 on the other results from both the Neogene (Pliocene–middle Miocene) and the early Eocene sequences being considerably thinner at Site 554.

Neogene sediments were deposited at two different accumulation rates (Fig. 9; Table 4). The uppermost 25 m of sediments representing the Pleistocene were deposited at a rate of approximately 1.7 cm/1000 yr. The second unit at Site 554 represents the Pliocene, the late Miocene, and the uppermost part of the middle Miocene (approximately 1.5 to 13.0 m.y. ago). The biostratigraphic data points in that time interval do not all fall on the suggested, linear, sedimentation curve. It is quite conceivable that some of these offsets reflect inaccurate biostratigraphic correlations between the different microfossil groups in use, or events in the correlation of marker fossils relative to the magnetic time scale. However, the rate of accumulation at Site 554 is distinctly low (0.7 cm/1000 yr.) in the Pliocene–middle Miocene interval, and since both the average Atlantic Ocean sedimentation rate (Davies et al., 1977) and the sedimentation rate established from the adjacent Site 116 (Laughton, et al., 1972) are higher by a factor of 4 (conservatively estimated) in the critical time interval, this suggests that bottom currents significantly influenced the mid-Neogene accumulation pattern at Site 554. Consequently, it appears reasonable to assume that the relatively small offsets in biostratigraphic data points relative to the suggested accumulation rate curve may represent fluctuations in rate of deposition rather than errors in biostratigraphic correlation. It thus follows that several unconformities of short duration probably occur in the mid-Neogene sequence, as well as several periods of more rapid accumulation, thereby giving rise to the spread of biostratigraphic data points. Finally, a linear sedimentation rate has been preferred to a curve which more precisely matches every biostratigraphic marker level, because the former type of curve is considered to represent the general character of the sedimentation process at Site 554.

A hiatus covering approximately 6 m.y. separates the upper middle Miocene strata from the underlying lower Miocene sequence. The lower Miocene is represented only by a few tens of centimeters of sediments.

The Oligocene and the upper Eocene are represented in a condensed, 12.5-m-thick sequence which spans approximately 15 m.y. The average net accumulation is thus extremely low (0.1 cm/1000 yr.). It is noteworthy that all nannofossil zones from NP25 to NP19/20 probably are represented in this condensed sequence.

A hiatus encompassing approximately 12 m.y. separates the late Eocene from the early Eocene. An 11-cm-thick manganese layer is present at the contact between the two stratigraphic units.

Compared to Sites 552 and 553, the lower Eocene sediments at Site 554 which overlie the sediment/basalt contact are thin. Because of the relatively small thickness, and the poor biostratigraphic control of the lower Eocene sediments at Site 554, it appears that the estimated accumulation rate of 0.5 cm/1000 yr. must be too low.

In conclusion, it is obvious that bottom currents have affected the Cenozoic sedimentation process at Site 554 in a far more drastic way compared to the effects observed in sediments recovered from Sites 552 and 553. This is in spite of the fact that several unconformities of considerable duration are present also in the two latter sites.

The sediments above the basalt at Site 554 are barren of nannofossils. The NP10/NP11 boundary occurs between 552A-5,CC and 5-4, in normally magnetized sediments interpreted to represent Anomaly 24B. This is consistent with results from Sites 553 and 555 (it should be noted, however, that this zonal boundary occurs stratigraphically slightly higher in Leg 81 sites than its true position shortly below Anomaly 24B; see Backman, this volume). It follows that the uppermost basalt at Site 554, and presumably also that at Site 552, are of a younger age than those encountered at Sites 553 and 555. The younger basalts at Site 552 and 554 appear to be of approximately the same age.

Accumulation Rates

The samples at this site are fairly widely spaced in time (Fig. 10; Table 5) but they show very clear trends. Apart from the high rate in the Pleistocene, the $CaCO_3$ accumulation rate is very uniform. However, the nannofossils and foraminifers show a reciprocal arrangement, with a nannofossil maximum in the late Miocene.

Comparison of Sites 552, 553, 554

The trends in the accumulation curves are shown on Figure 11. Hole 552A serves as a detailed reference with which to compare Sites 553 and 554. Several interesting points are evident.

The middle–early late Miocene accumulation rates for both nannofossils and foraminifers are very uniform at

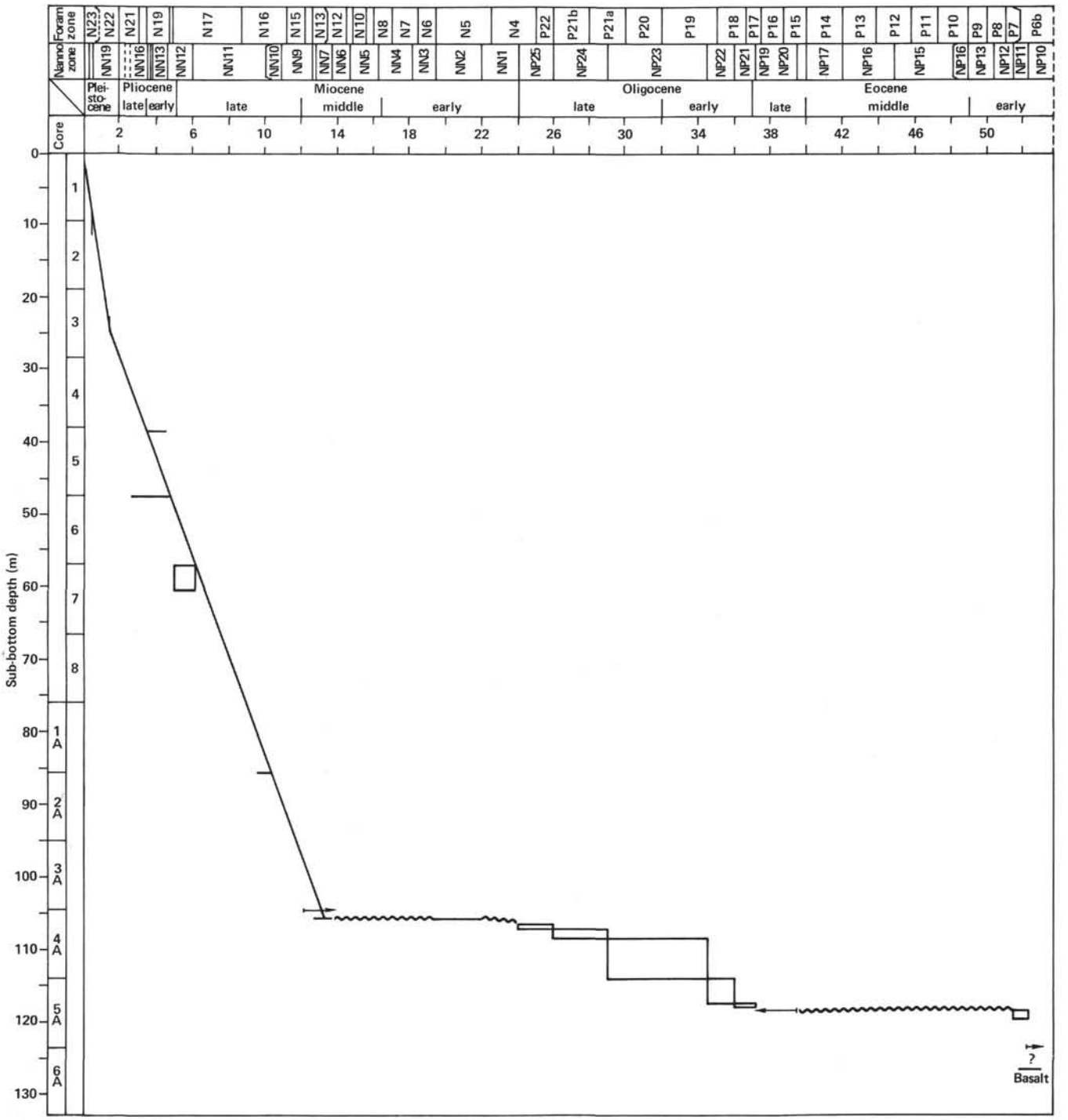

Figure 9. Sedimentation rates, Site 554.

all three sites. This could indicate uniformity of production rates or similarity of depositional regimes.

The high nannofossil and foraminiferal accumulation rates of the post-Oligocene section (contourities, see site chapters, Sites 552, 553) are very similar in both Sites 552 and 553. However, Site 554 shows such a uniform rate throughout that it clearly was not under the influence of contour current deposition.

In the glacial Pliocene–Pleistocene the accumulation rates were lower at Site 554 than at Site 552, except in the uppermost part where the relationship is reserved.

ORGANIC GEOCHEMISTRY

Site 554 contains very little organic carbon (OC) (0.02 to 0.11%) even relative to the other sites (see Table 6 and Fig. 12).

Table 4. Biostratigraphic data used to derive sedimentation rates for Site 554 (see also Fig. 9).

Paleontologic event	Depth (m)	Million years ago	Sedimentation rate (cm/1000 yr.)
L. O. *P. lacunosa*	9.5–11.5	0.458	1.8
L. O. *C. macintyrei*	24–25.5	1.45	
Co-occurrence *R. pseudoumbilica, C. rugosus*	38.5	3.53–4.57	
L. O. *D. quinqueramus*	54–57	6.0	
N. jouseae present	47.5	2.65–4.5	0.7
T. miocenica present	57–60.5	5–6.2	
lowermost NN11	85.5	~9.6–10.3	
G. mayeri present	104.5	>12.2	
NN7/NN8	105.5	12.6–13.8	———
Co-occurrence *S. belemnos, T. carinatus*	106	19.4–22	———
NP25	106.5–107	24–26	
NP24	107–108.5	26–29	
NP23	108.5–114	29–34.5	
NP22	114–117.5	34.5–36	<0.1
NP21	117.5–118	36–37.2	
NP 19/20	118.6	<39.5	———
NP11	118.6–119.5	51.4–52.3	>0.5
NP10	123.5	>52.3	———

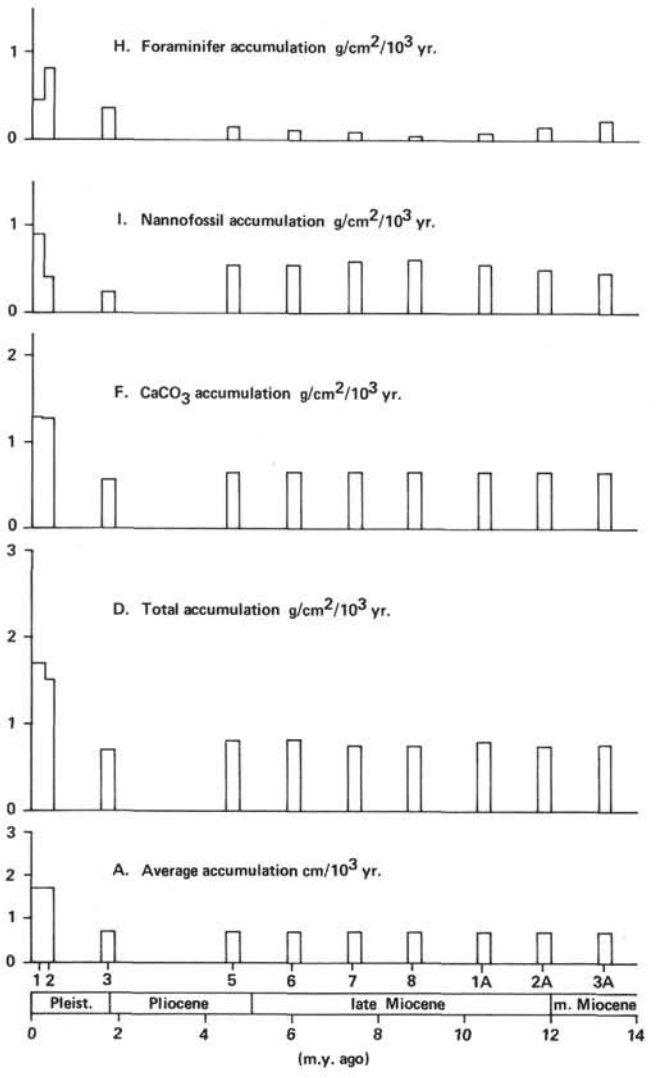

Figure 10. Neogene sediment accumulation rates, Holes 554 and 554A. (See Site 552 for explanation of lettering A to H).

Table 5. Data for sediment accumulation rates (see also Fig. 10).

Core	A	B	C	D	E	F	G	H	I	J
Hole 554										
1,CC	1.7	1.636	0.98	1.7	76	1.29	14.94	0.42	0.87	0.41
2,CC	1.7	1.584	0.91	1.5	75	1.28	31.85	0.86	0.42	0.22
3,CC	0.7	1.62	1.0	0.7	82	0.57	30.68	0.35	0.22	0.13
5,CC	0.7	1.72	1.17	0.82	95	0.66	10.00	0.12	0.54	0.28
6,CC	0.7	1.762	1.16	0.81	92	0.64	7.82	0.10	0.54	0.21
7,CC	0.7	1.693	1.07	0.75	94	0.66	6.45	0.08	0.58	0.17
8,CC	0.7	1.693	1.07	0.75	93	0.65	2.94	0.03	0.62	0.10
Hole 554A										
1,CC	0.7	1.731	1.15	0.80	91	0.64	5.48	0.07	0.57	0.16
2,CC	0.7	1.656	1.06	0.74	92	0.64	11.11	0.13	0.51	0.10
3,CC	0.7	1.719	1.10	0.77	91	0.64	17.37	0.21	0.43	0.13

Note: For key to letters see Site 552 accumulation rates.

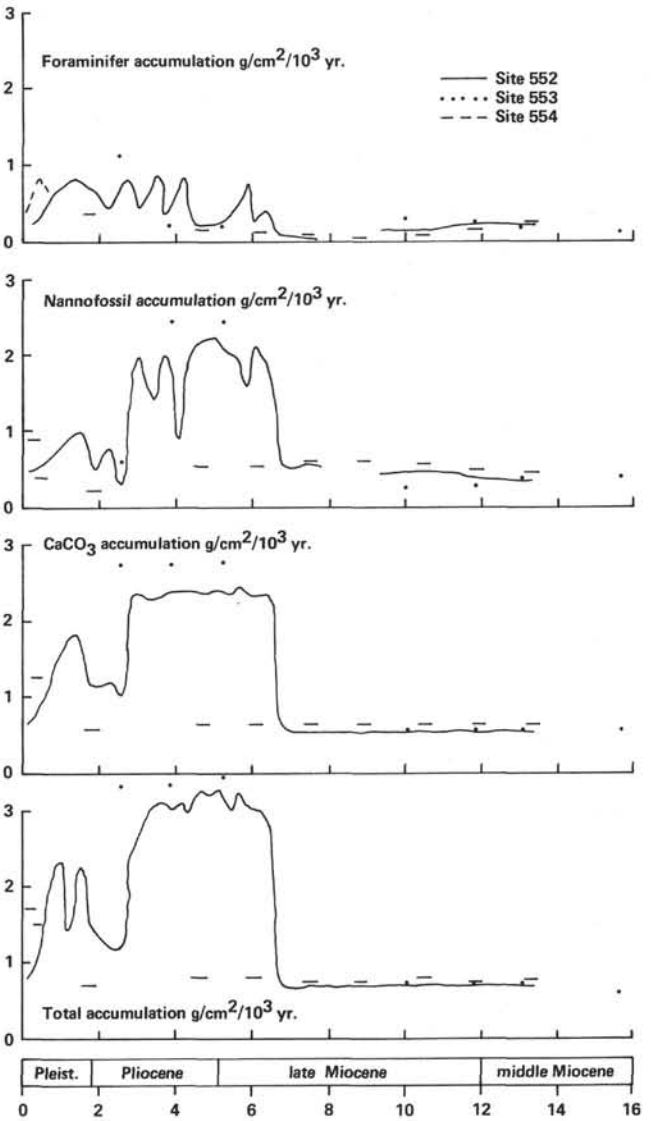

Figure 11. Comparison of Neogene sediment accumulation rates, Sites 552 through 554.

Table 6. Pyrolysis data, Site 554.

Sample (interval in cm)	S_1 (mg HC / g rock)	S_2 (mg HC / g rock)	S_2 (T_{max} °C) Peak A	Peak B	S_3 (mg CO_2 / g rock)	$S_1 + S_2$ (mg HC / g rock)	$S_1 / (S_1 + S_2)$	S_2/S_3	HI (mg HC/g OC)	OI (mg CO_2/g OC)	Remarks
Hole 554											
1-4, 133-135	0.07	0.02	—	—	1.38	0.09	0.78	0.02	67	4600	56% $CaCO_3$, tan, Pleistocene
5-6, 135-137	0.04	0.03	—	—	0.87	0.07	0.57	0.03	75	2900	97% $CaCO_3$, ooze, white, e. Pliocene
7-4, 119-121	0.11	0.04	—	—	0.73	0.15	0.73	0.06	50	913	91% $CaCO_3$, l. Miocene
Hole 554A											
3-2, 110-112	0.05	0.02	—	—	0.77	0.07	0.71	0.03	50	1925	91% $CaCO_3$, m. Miocene
5-2, 5-7	0.07	0.02	—	—	0.92	0.09	0.78	0.02	50	2300	81% $CaCO_3$, Oligocene, above Mn unconformity layer
5-5, 13-15	0.17	0.35	344	(444)?	1.91	0.52	0.33	0.18	318	1736	9% $CaCO_3$, SS., e. Eocene just below unconformity
6-2, 120-122	0.12	0.06	—	—	0.46	0.18	0.67	0.13	300	2300	62% $CaCO_3$, SS., calcite cement?; top of basalt; e. Eocene

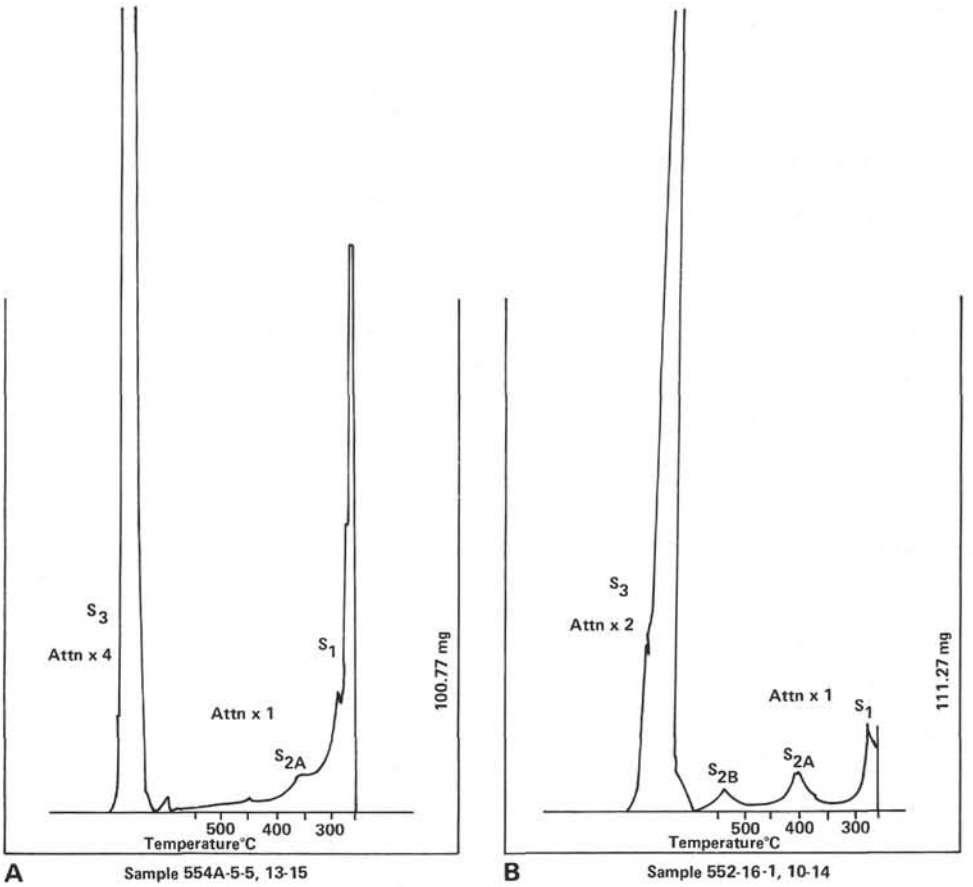

Figure 12. Pyrolysis analysis comparison, Sites 552 and 554.

Gases

There were no C_1–C_4 hydrocarbons detectable in the sediments from Site 554. The lower detection limit of the method is 0.04 ppm of C_1 and 0.01 ppm of C_2–C_4. The absence of high hydrocarbons is not unreasonable considering the very low levels of highly oxidized organic matter present.

Sediments

The amount of pyrolyzable organic matter is consistently low in the Recent to Oligocene sediments. The

type III matter present is highly oxidized (see Hole 553B), and a highly oxidized marine origin is suggested by the S_2/S_3 ratio (0.02–0.06) and the character of the pyrolysis scans (see Table 6). The ratio suggests that a significant amount (70%) of the total hydrocarbons derived possibly from the sedimentary organic matter exist as "free hydrocarbons." This suggests a marine source of organic matter (OM) which is readily converted to hydrocarbons under mild conditions (low temperature decomposition). However, it is not known to what extent this relationship holds in view of the large oxygen–carbon component of organic matter present. It should also be cautioned that this ratio can indicate possible contamination, or migrated hydrocarbons.

The gradual decrease in the S_3 (oxygen–carbon organic matter) component down section (Present to middle-Miocene) suggests decompositional loss of hydrophilic groups (OH, COOH, OCH_3, C=0) similar to Hole 553B.

As in the previous sites, Sites 552 and 553, the Oligocene and Eocene sediments show an increase in organic matter, as a result of significantly different environmental conditions (shallow marine) and the close proximity of a terrestrial source. However, the most distinctive feature of Site 554 is the absence of the very mature (550°C) component of organic matter seen so distinctly at Sites 552 and 553. Figure 12 shows comparative pyrolysis scans of Eocene samples from Site 552 (12A) and Site 554 (12B). The absence of this very mature component (probably terrestrial reworked or volcanogenically matured) coincides with an absence of detrital heavy minerals and suggests a different source of organic matter at Site 554.

In summary, the low (0.4% OC) levels of sedimentary organic matter at Site 554 are type III (highly oxidized marine?) from the Oligocene to the Present, indicating a deep marine environment similar to the present. The Eocene sediments show an increase in organic matter (0.11%), with a source distinct from that at Sites 552 and 553. A fuller discussion is given elsewhere in this volume (Kaltenback et al.).

BASALT LITHOLOGY

Hole 554A first encountered basalt at 126.75 m subbottom in Core 6-3 at 25 cm, and the hole ended in basalt at 209.0 m total depth (Core 14). Within this interval of 82.25 m, the basaltic lava flows are interbedded with sandstones and conglomerates derived from disintegration of the flows by marine processes. Total recovery rate for this was only 16%, and this comprises 8.95 m of basalt and 4 m of sediment. Based on the number of sediment interbeds and the basalt texture at least six flows are present in the section cored (see Table 3).

In general the basalt is aphyric, gray in color (10YR 5/1 or 2.5Y 6/0), and moderately altered, with dark brown (7.5YR 4/4) and greenish-gray (5G 6/1) palagonite rims common at the upper and lower margins of flows. Fracturing throughout the flows has contributed to the internal alteration of the basalt. This can be seen as 1-cm-wide alteration zones (often pale brown, 10YR 6/3) on either side of nearly all fractures. The vertical and horizontal fracturing has resulted in the basalt breaking into blocks a few centimeters in size. Most fractures are less than 2 mm wide and are filled with smectite and in some cases a late phase of calcite. Sediment and palagonite breccia has infilled some wider (about 2 cm) fractures, indicating that the fractures allowed seawater to circulate into the basalt. The only relatively fresh basalt occurs in the central cores between fractures and in the less vesicular portion of the thicker flows (Sections 7-3 and 14-1). The upper margins of some flows lack a glassy or palagonite rind, perhaps because of submarine erosion. No obvious pillows were observed. However fragments (1 to 5 mm) of angular palagonite and basaltic glass are abundant on the top and at the base of other flows and in the fractures (between pillows?) at the top of the flow. This palagonite breccia is cemented by calcite and probably is a hyaloclastite deposit.

The basalt is usually very vesicular near the top of the flow, with large (up to 1.5 cm) irregular vesicles common. Most of the vesicles are empty or lined with only a thin layer of dark green smectite (for example, Sections 7-1 and 2). Even the smaller (1–2 mm) spherical vesicles are generally empty; some are filled with smectite or smectite followed by calcite spar and rarely zeolite (phillipsite). Some of the vesicles exhibit vertical elongation and are not evenly distributed across the width of the core. A few very irregular large "vesicles" are filled with micritic calcite, with palagonite clasts suspended in the micrite. This suggests that the micrite may be soft calcareous sediment incorporated into the flow and now recrystallized.

Eight thin sections were examined and show that the basalt is aphyric (fine-grained) and consists of unaltered plagioclase (labradorite) and clinopyroxene (augite), with a groundmass of glass comprising 15 to 25% of the rock. Minor phases include magnetite and very rare olivine (mostly altered to iddingsite). This mineralogy was confirmed by XRD. The interstitial glass in the basalt from flow interiors is fresh, whereas the glass near the flow margins is altered to smectite and palagonite.

The top 5 m of Core 7 probably represent one flow unit, with very fine-grained vesicular basalt grading down into a more passive, less vesicular and slightly coarser basalt, a thin vesicular zone and chilled palagonitized margin occurs at the base in Section 4. The massive interval does contain subhorizontal streaks (discontinuous fractures?) now composed of dark smectite. The basalt is most altered at the top and base of the flow. No pillows are preserved intact, although broken pillow segments are common in the interbedded conglomerates. These clasts (up to 5 cm in size) show well-defined curved glassy margins (one-half to 1 cm thick) which are in various stages of alteration to palagonite.

The less vesicular basalt recovered does contain rare inclusions or clasts (2 to 5 cm) of very vesicular finer-grained basalt, which are more altered and have indistinct (resorbed?) margins.

In conclusion the section recovered is characterized by the abundance of well-developed palagonite and the internal alteration of the basalt along fractures to smec-

tite and rate phillipsite, followed by the infilling of some fractures filling with sedimentary clasts and calcite cementation.

The evidence indicates that these basalts were submarine flows subject to low-temperature alteration at the seafloor for a relatively long time before being broken up by wave action to form the overlying conglomerate.

PHYSICAL PROPERTIES

Physical properties measured on sediments, basalts, and intercalated sediments recovered in Holes 554 and 554A include compressional-wave velocity, 2-minute GRAPE wet-bulk density, continuous GRAPE wet-bulk density, and wet-bulk density, wet-water content, and porosity by gravimetric techniques.

The gravimetric measurements were carried out in the shipboard chemistry laboratory.

Shear strength measurements were not carried out because the soft sediments were severely disturbed throughout the recovered material.

All other measurements and calculations were carried out as described in the Introduction and Explanatory Notes. The data and calculations of the sediments to a depth of 126.6 m should be treated with caution because of the above-mentioned drilling disturbances.

All the physical property data measured and calculated are given in Table 7 and plotted in Figure 13.

Main Results

The upper three lithologic units described cannot be distinguished from the physical property data. The sonic velocity and the calculated acoustic impedance vary only slightly (see the physical properties correlation chart), and the other data do not show reliable changes or trends. The sonic velocity averages approximately 1.55 km/s, and porosites range between 56.5 and 68.2%, which is quite typical for predominantly nannofossil and foraminifer-nannofossil oozes. These late Eocene to Quaternary sediments are here named Unit A.

The first remarkable increase in the sonic velocity (2.04 km/s and the resulting increase in the acoustic impedance (3.42 $[g/cm^2 \cdot s)]10^5$) was measured on sediments from 119.63 m depth and coincides with the first occurrence of the zeolitic tuffaceous sediments and the zeolitic tuffs. These volcaniclastic sediments of early Eocene age belong to Unit B and are 7.80 m thick. The lower boundary (at 126.60 m) defines the top of the basalts and volcanogenic conglomerates which were penetrated to total depth.

Although the recovery in the interval (Unit C) between 126.60 m and total depth (209 m) is very poor, three different rock types can be characterized by their physical properties:

1. Dense fine-grained basalts with sonic velocities above 5 km/s and grain densities of about 3.05 g/cm^3;
2. Vesicular basalts characterized by sonic velocities of about 4.5 km/s. The densities are similar to the above basalts, but the porosity results in higher water contents; and
3. Intercalated sediments with sonic velocities ranging from 3.7 to 4.5 according to pebble size and degree of cementation.

Table 7. Physical property data, Holes 554 and 554A.

Sample (Interval in cm)	Depth in hole (m)	Sound velocity			GRAPE "Special" wet-bulk density 2-min. count (g/cm^5)		Gravimetric			
		Beds (km/s)	Beds (km/s)	Temp (°C)	∥Beds	⊥ Beds	Wet-bulk density (g/cm^3)	Wet-water content Salt Corr. (%)	Porosity (%)	Acoustic impedance ($g\ 10^5$) × ($cm^2 s$)
Hole 554										
2-2, 134-136	12.36	1.571		19.0	1.636		1.62	39.93	64.68	2.57
2-4, 137-137	15.39	1.491		19.0	1.487		1.51	46.77	70.83	2.22
2-5, 102-104	16.54	1.581		19.0	1.526		1.62	41.49	67.13	2.413
2-6, 65-67	17.67	1.564		19.0	1.584		1.56	42.69	66.77	2.477
3-4, 57-59	24.09	1.537		19.0	1.575		1.58	43.15	68.19	2.421
3-5, 141-143	26.43	1.608		19.0	1.62		1.65	38.39	63.21	2.605
5-3, 102-104	42.04	1.549		19.0	1.788		1.74	32.51	56.51	2.770
5-5, 100-102	45.02	1.555		19.0	1.72		1.76	32.01	56.43	2.675
6-5, 119-121	54.71	1.544		19.0	1.664		1.70	36.88	62.77	2.57
6-6, 79-81	55.81	1.565		19.0	1.762		1.75	34.22	60.03	2.758
8-3, 77-80	70.30	1.51		19.0	1.693		1.66	36.72	61.07	2.556
Hole 554A										
2-1, 87-0	86.40	1.519		19.0	1.731		1.75	33.56	58.89	2.629
2-2, 83-86	87.86	1.512		19.0	1.656		1.72	35.67	61.34	2.459
3-2, 91-93	97.43	1.504		19.0	1.693		1.66	37.04	61.47	2.546
3-3, 132-134	99.34	1.537		19.0	1.719		1.70	36.26	61.55	2.642
4-1, 117-119	105.69	1.537		19.0	1.645		1.66	37.58	62.43	2.528
4-3, 85-87	108.37	1.571		19.0	1.642		1.62	39.80	64.50	2.58
5-1, 51-53	114.53	1.514		19.0	1.646		1.63	39.12	63.94	2.492
5-3, 60-62	117.62	1.588		19.0	1.742		1.60	37.93	60.63	2.766
5-4, 111-113	119.63		2.037	19.0		1.680	1.70	36.45	61.82	3.422
6-2, 46-48	125.48		2.30	19.0		1.884	1.89	26.03	49.28	4.347
6-3, 29-31	126.81		4.388	19.0		2.306				10.119
7-1, 87-89	133.89		4.583	19.0		2.188	2.66	6.35	16.90	10.028
7-2, 54-56	135.06		5.022	19.0		2.525	2.79	4.62	12.89	12.681
7-3, 113-115	137.15		5.237	19.0		2.583	2.96	1.94	5.74	13.527
7-4, 91-93	138.43		3.763	19.0		2.289	2.40	11.13	26.71	8.614
8-1, 92-94	143.42		5.607	19.0		2.514	2.83	3.58	10.14	14.096
8-2, 106-108	145.06		4.653	19.0		2.49	2.89	5.87	15.42	11.577
9-1, 95-37	152.05		5.68	19.0		2.49	2.79	4.52	12.60	12.879
10-1, 45-47	161.05		5.142	19.0		2.47	2.83	3.79	10.73	12.721
11-1, 3-5	171.03		4.601	19.0		2.40	2.69	6.29	16.88	11.029
14-1, 50-52	200.00		5.212	19.0		2.61	2.85	2.69	7.66	13.624

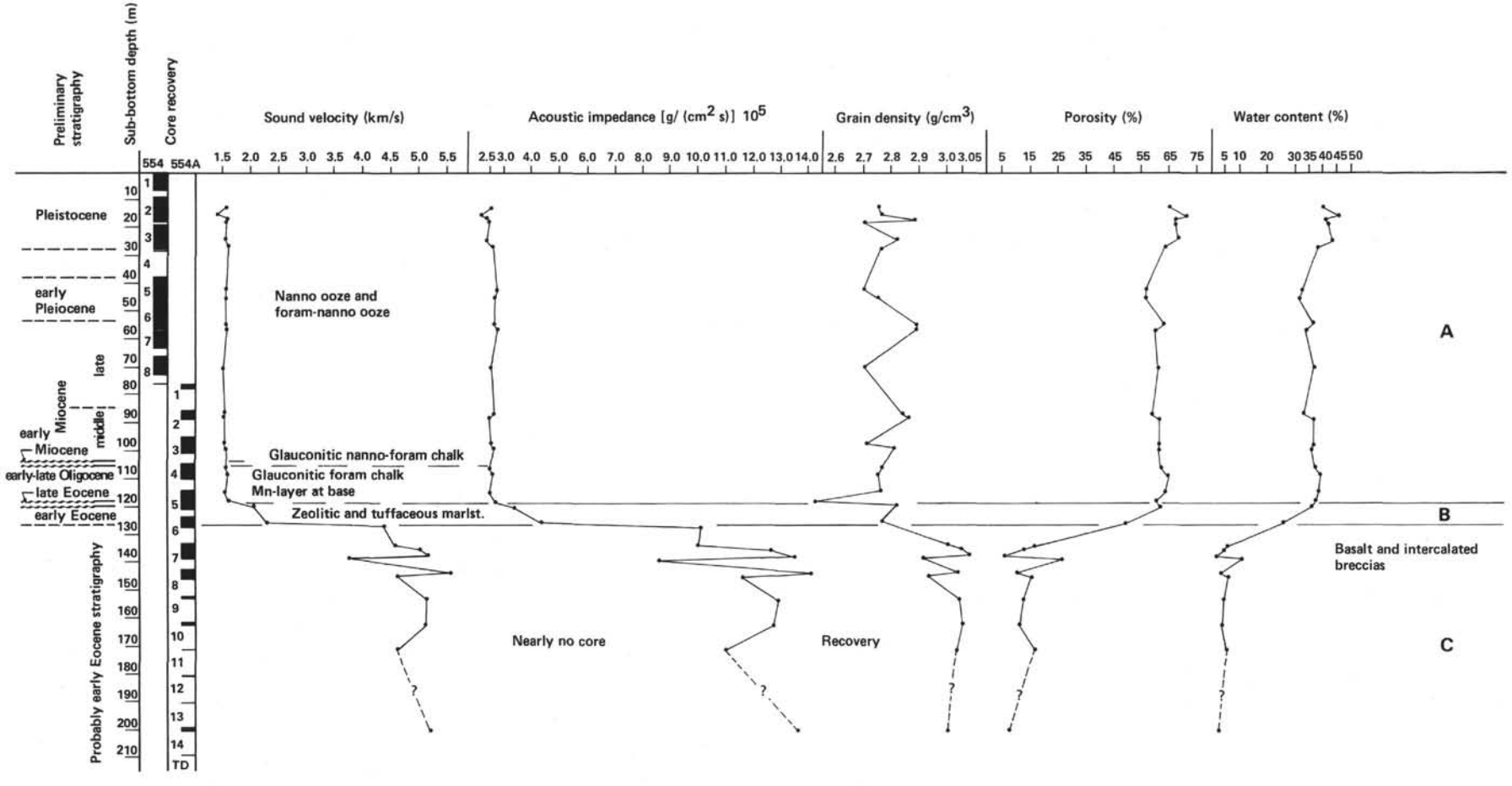

Figure 13. Physical properties correlation chart, Site 554 (1:1000). (See text for explanation of A, B, C.)

The physical property data obtained at Site 554 support our interpretation of the seismic section.

CORRELATION OF SEISMIC REFLECTORS WITH DRILLING RESULTS

Site 554 was located on the "outer high" separating the dipping reflector sequence from the adjacent ocean crust (see Background and Objectives). The final site was located close to SP 1150 on IFP-CEPM line RH-115 (Fig. 3). These data were acquired using a Vaporchoc sound source at a depth of 6 m and a 24 trace streamer. The line was stacked, but processing was confined to a linear dynamic correction and time varied filtering. Velocity analyses were made at 5 km intervals. Additional data include the single channel airgun section taken by *Glomar Challenger* while crossing the site and a new 60 channel seismic line (IOS-6) recently obtained by IOS using Maxi-pulse. The latter data have not yet been fully processed.

Correlation of Seismic Reflections at Site 554

At Site 554, the first clear reflection appears at 0.16 s (two-way time) as an event with a gentle eastward dip (Fig. 3). Beneath the reflection, only diffractions are present, and any coherent reflections are either absent or totally obscured by these events. To the southeast the reflection drops down sharply by 0.2 s. In this region, the strong reflector is clearly unconformable with the underlying westward dipping reflectors. These do not apparently continue westward beneath the strong reflector at Site 554, but diffraction migration will be necessary to establish this conclusively.

No logs could be run at Site 554, and correlation of the lithostratigraphy is here made using the physical properties data. Taking a mean velocity of 1.5 km s^{-1} for the sediments above the basalts at 126.50 m, a two-way time of 0.16 s is found. This traveltime is in excellent agreement with the strong reflector at 0.16 s, which thus corresponds to the top of basaltic breccia and basaltic flows of Unit V.

SUMMARY AND CONCLUSIONS

The structure and topography of the west margin of Rockall Plateau was briefly described and summarized in the Site 553 chapter in terms of three units (Figs. 2 and 3).

The shallowest and most landward of these are the Hatton and Edoras banks. The second unit is present at the base of the steep slope to the west of the banks and has been previously called the Edoras Basin. This unit is characterized by the prominent series of dipping reflectors drilled at Sites 552 and 553.

The third and most oceanward of these units is called the outer high and is situated 40 to 50 km west of the steep slope bounding the Hatton and Edoras banks. The outer high trends parallel to and partly overlaps the oldest magnetic anomaly (24B) recorded in the adjacent ocean crust. The topographic expression of the outer high varies along its length. In the north it is a prominent flat-topped ridge on which sediments are thin to absent. The ridge plunges southward so that the original relief is lost beneath the increasing sediment cover. However, on the control seismic profile (Fig. 2), the outer high remains evident as a prominent feature defined by a strong flat-lying reflector that apparently merges with the oceanic basement to the west. No coherent seismic reflectors can be discerned beneath the high.

Similar ridges generally called outer highs have been observed in equivalent structural positions on many passive margins and have been interpreted in various ways. One hypothesis is that the high is the eroded crest of a fault block; others propose that the outer high represents either the first oceanic crust or an uplift developed during the terminal part of the rifting phase (see Background and Objectives section). In the case of the Rockall margin, the presence of a thin sedimentary section overlying the outer high made the site ideally suited to penetrate the basement forming the high at shallow depth and to test these models.

Site 554 was located on the outer high near SP1150 on line IFP-CEPM RH115.

Basalt Lava Flows and Interbedded Sediments

A total of 82.60 m of interbedded basalt lava flows, volcanogenic sandstones, and conglomerates were recovered between 126.60 and 209 m depth (82.60 m thickness) (Unit V or Fig. 8). The top of this sequence corresponds to the reflector defining the crest of the outer high.

Recovery in this sequence was particularly poor (10%) and the exact proportions of sediment and basalt must remain unknown, although at least six flows are apparently present in this interval. The flows are typically rimmed with palagonite. No obvious pillows were seen, but broken pillow fragments are common in the breccia infilling the fractures in the basalt as well as in the interbedded conglomerates. These show well-defined glassey margins altered in various degrees to palagonite. The palagonite breccia infilling fractures is probably a hyaloclastite.

Shipboard thin-section examination of the basalt shows an aphyric texture consisting of unaltered labradorite and augite, with a glassy groundmass comprising some 15 to 25% of the rocks: magnetite and rare olivine showing alteration to iddingsite are minor phases. Glass in the interior of the flows is fresh, whereas glass near the margins is typically altered to smectite and palagonite. Vesicles that are typically empty decrease in abundance downflow and are lined with smectite; where filled, smectite and calcite spar are present. Micritic calcite in which palagonite clasts are interspersed may represent recrystallized soft sediment that has been incorporated in the flow. Sonic velocities in the basalts ranged from 4.5 km s^{-1} (vesicular basalt) to more than 5 km s^{-1} (dense fine-grained basalts). The interbedded sediments are volcanogenic conglomerates and sandstones. The conglomerate consists of rounded to angular clasts of basalt, highly altered basalt, and palagonite cemented by calcite spar. Characteristic features of the sandstones and conglomerates are: the lack of a clay matrix or any other terrigenous detritus, the uniform basaltic composition of the clasts, absence of any sedimentary structures, and lack of bioclastic carbonate. The contact

with the underlying basalt is sharp, and the lack of a palagonitic or glassy margin is suggestive of erosion. Some sand has penetrated fractures in the underlying basalt. The characteristics of the basalts are compatible with eruption in a submarine environment followed by low temperature alteration. The succeeding interbedded sands and conglomerates suggest that their deposition might have taken place in a high-energy littoral environment.

The basalts and the overlying sediments show normal polarity after demagnetization. Reverse polarity on one sample has also been detected in the lower part of the basalt sequence. A reversed polarity interval recorded within the normal interval may have been measured on a basalt boulder. The conglomerate random-distribution test carried out on these boulders shows that the basalts have very stable magnetization. These preliminary shipboard measurements are subject to revision after further demagnetization onshore (Krumsiek and Roberts, this volume).

Early Eocene

A thin (7.8 m) interval of early Eocene (NP10? to NP11) zeolitic tuffs and tuffaceous marlstones overlies the conglomerate. The tuffaceous component consists of green lapilli, palagonitized glass, and a mixture of Fe-smectites and phillipsite that may have formed by the *in situ* devitrification of volcanic glass. No heavy minerals were found in contrast to the section of equivalent age at Site 553. Downward mixing of late Eocene sediments by bioturbation is observed to a depth of 35 to 40 cm below the manganese layer forming the base of the late Eocene sediments. Siliceous fossils are absent, perhaps reflecting a combination of low productivity and dissolution, although low productivity is not indicated by the calcareous microfossils. Depths of deposition indicated by benthic foraminifers range from 75 to 125 m in the lower part of the section to 100 to 150 m in the overlying sediments. The organic geochemistry suggests increased production of marine organic matter, which is highly oxidized and a lack of the reworked terrestrial matter found at other sites (see Organic Geochemistry section).

Late Eocene

A thin late Eocene (80 cm) interval forms the basal part of a late Eocene to early Miocene condensed sequence. The late Eocene is separated from the underlying early Eocene by an 11-cm-thick manganese rich layer. Burrows in the underlying early Eocene sediments contain only late Eocene sediment. This indicates that the middle Eocene was either not deposited at the site or that pre-late Eocene erosion took place removing the NP12–NP18 interval completely. The manganiferous layer may indicate that an incipient hard ground developed during the missing interval. The late Eocene sediments are glauconite-rich foraminiferal chalks to marls in which planar and cross laminae are common as well as syndepositional microfaulting. Deposition may have taken place in epibathyal depths of greater than 700 m.

Oligocene

The Oligocene section is about 11.65 m thick, and all the zones of the Oligocene are apparently represented. The Oligocene consists of interbedded foraminiferal marls and foraminiferal chalks becoming less glauconitic upward. Minor but persistent components are radiolarians, sponge spicules, and fish debris, which are more abundant than above. Depths of deposition were greater than 700 m.

Early Miocene

The early Miocene (NN2) of approximately 25 cm thickness consists of glauconite-rich foraminiferal chalk resting with a sharp uneven contact on the underlying Oligocene. The sharpness of the contact suggests that a hiatus may be present. Depths of deposition were greater than 2200 m.

Middle Miocene to Early Pliocene (77.50 m thick)

The unconformity representing a hiatus of about 6 m.y. separates the middle Miocene from the underlying early Miocene sediments. The middle Miocene sediments are bluish white to gray foraminifer-nannofossil oozes that show faint color cycles and are interbedded with chalk. The disappearance of chalk upward marks the top of the middle Miocene. The overlying late Miocene to early Pliocene sediments consist of bluish-white foraminifer-nannofossil or nannofossil-foraminiferal oozes showing fine laminae. The benthic foraminiferal assemblages indicate depths of deposition of 2200 to 2900 m throughout middle and late Miocene and late Pliocene time.

Sediments accumulated at an average rate of 0.7 cm/1000 yr. during this interval. The biostratigraphic data points used to determine this rate do not all fall on a straight line (see Sedimentation Rates section). One explanation may be the presence of several unconformities in the Neogene sequence of short duration separated by periods of more rapid sediment accumulation.

Pleistocene (28.5 m thick)

A possible unconformity representing a hiatus encompassing part of Zone NN19 is present. The Pleistocene section comprises alternating beds of white to light yellowish-brown nannofossil-foraminiferal oozes or white foraminiferal oozes.

REFERENCES

Boillot, G., et al., 1980. Ocean continent boundary off the Iberian margin: A serpentinite diapir west of Glaicia Bank. *Earth Planet. Sci. Lett.*, 48(1):23–24.

Burckle, L. H., 1972. Late Cenozoic planktonic diatom zones from the eastern equatorial Pacific. *First Symp. Recent and Fossil Marine Diatoms*, 39:217–246.

_____, 1977. Pliocene and Pleistocene diatom datum levels from the equatorial Pacific. *Quat. Geol.*, 7:330–340.

Burckle, L. H., and Trainer, J., 1979. Middle and late Pliocene diatom levels from the central Pacific. *Micropaleontology*, 25(3):281–293.

Davies, T. A., Hay, W. W., Southam, J. R., and Worsley, T. R., 1977. Estimates of Cenozoic sedimentation rates. *Science*, 197(4298):53–55.

Featherstone, P., Bott, M. H. P., and Peacock, J. H., 1977. Structure of the continental margin of southeastern Greenland. *Geophys. J.*, 48(1):15–27.

Foreman, H. P., 1975. Radiolaria from the North Pacific, Deep Sea Drilling Project, Leg 32. *In* Larson, R. L., Moberly, R., et al., *Init. Repts. DSDP*, 32: Washington (U.S. Govt. Printing Office), 579–676.

Groupe Galice, 1979. The continental margin off Galicia and Portugal: Acoustical stratigraphy, dredge stratigraphy and structural evolution. *In* Sibuet, J.-C., Ryan, W. B. F., et al., *Init. Repts. DSDP*, 47, Pt. 2: Washington (U.S. Govt. Printing Office), 633–662.

Grow, J., and Sheridan, R. E., 1981. Deep structure and evolutions of the continental margin off the eastern United States. *Geology of Continental Margins* (Int. Geol. Cong. 26th, Paris). *Oceanol. Acta*, 4:11–19.

Hinz, K., 1981. A hypothesis on terrestrial catastrophes wedges of very thick oceanward dipping reflectors beneath passive continental margins. *Geol. Jahrb.*, E22:3–28.

Jones, M. T., and Roberts, D. G., 1975. Magnetic anomalies in the northeast Atlantic. *First Mtg. European. Geol. Soc. Reading*. (Abstract)

Laughton, A. S., Berggren, W. A., et al., 1972. *Init. Repts. DSDP*, 12: Washington (U.S. Govt. Printing Office).

Montadert, L., Roberts, D. G., de Charpal, O., and Guennoc, P., 1979. Rifting and subsidence of the northern continental margin of the Bay of Biscay. *In* Montadert, L., Roberts, D. G., et al. *Init. Repts. DSDP*, 48: Washington (U.S. Govt. Printing Office), 1025–1060.

Müller, C., 1979. Calcareous nannofossils from the North Atlantic (Leg 48). *In* Montadert, L., Roberts, D. G., et al., *Init. Repts. DSDP*, 48: Washington (U.S. Govt. Printing Office), 589–640.

Naini, B., and Talwani, M., 1981. Structural framework and the evolutionary history of the continental margin of western India. *Hedberg Conf. Am. Assoc. Pet. Geol.*, p. 43. (Abstract)

Riedel, W. R., and Sanfilippo, A., 1978. Stratigraphy and evolution of tropical cenozoic radiolarians. *Micropaleontology*, 24:61–96.

Roberts, D. G., Montadert, L., and Searle, R. C., 1979. The western Rockall Plateau: Stratigraphy and structural evolution. *In*. Montadert, L., Roberts, D. G., et al., *Init. Repts. DSDP*, 48: Washington (U.S. Govt. Printing Office), 1061–1088.

Scheupbach, M., and Vail, P. R., 1980. Evolution of outer highs on divergent continental margins. *Continental Tectonics*: Washington, D.C. (Natl. Acad. Sci.), pp. 50-61.

Shipboard Scientific Party, 1972. Sites 116 and 117. *In* Laughton, A. S., Berggren, W. A., et al. *Init. Repts. DSDP*, 12: Washington (U.S. Govt. Printing Office), 395–672.

Talwani, M., Konig, and Mutter, J. C., 1979. The coastal structure and evolution of the area underlying the magnetic quiet zone of the margin south of Australia. *In* Watkins, J. S., et al. (Eds.), *Geological and Geophysical Investigations of Continental Margins. Mem. Am. Assoc. Pet. Geol.*, 29:161–175.

Vierbuchen, R., Vail, P. R., and George, R. P., 1981. A possible mechanism for the formation of outer highs on passive margins. *AAPG Hedberg Conf.*, p. 63. (Abstract)

APPENDIX
Smear Slide Summary, Holes 554 and 554A

TRACE	t
<5%	RARE
5–25%	COMMON
25–50%	ABUNDANT
>50%	DOMINANT

Dominant Lithology

Core-Section (interval in cm)	BIOGENIC COMPONENTS							NON-BIOGENIC COMPONENTS								AUTHIGENIC COMPONENTS									
	Forams	Nannofossils	Radiolarians	Diatoms	Sponge Spicules	Fish Debris	Silico-flagellates	Quartz	Feldspars	Heavy Minerals	Light Glass	Dark Glass	Glauconite	Clay Minerals	Other lithic (Specify)	Palagonite	Zeolites	Amorphous Iron Oxides	Fe/Mn Micro Nodules	Pyrite	Recrystal. Silica	Carbonate (unspecified)	Carbonate Rhombs	Other (specify)
1-1, 40				t																					
1-1, 76					t																				
1-6, 46			t	t																					
2-2, 45												t													
2-3, 94																						t			
2-5, 110			t																						
3-2, 26					t																				
3-4, 60																			t						
3-6, 89										t		t				t									
5-4, 74								t																	
6-5, 57					t																				
7-3, 70					t																				
8-4, 70			t	t	t																				

Hole 554A

1,CC			t			t									t										
2-2, 70				t		t					t						t								
3-3, 93			t						t	t					t							t			
3-3, 120						t			t																
3-4, 52			t																						
4-2, 22			t								t						t								
4-3, 69						t																			
4-3, 106			t			t													t						
5-1, 100					t	t											t						t		
5-2, 109					t																				
5,CC					t																				
6-1, 55																									
6-2, 70																									
6-2, 123						t																			

Minor Lithology

Hole 554

2-3, 37																			t						
6-5, 142																									
6-6, 32							t																		

Hole 554A

5-3, 139																									
6-3, 18																									

SITE 554 HOLE CORE 1 CORED INTERVAL 0.0–9.5 m

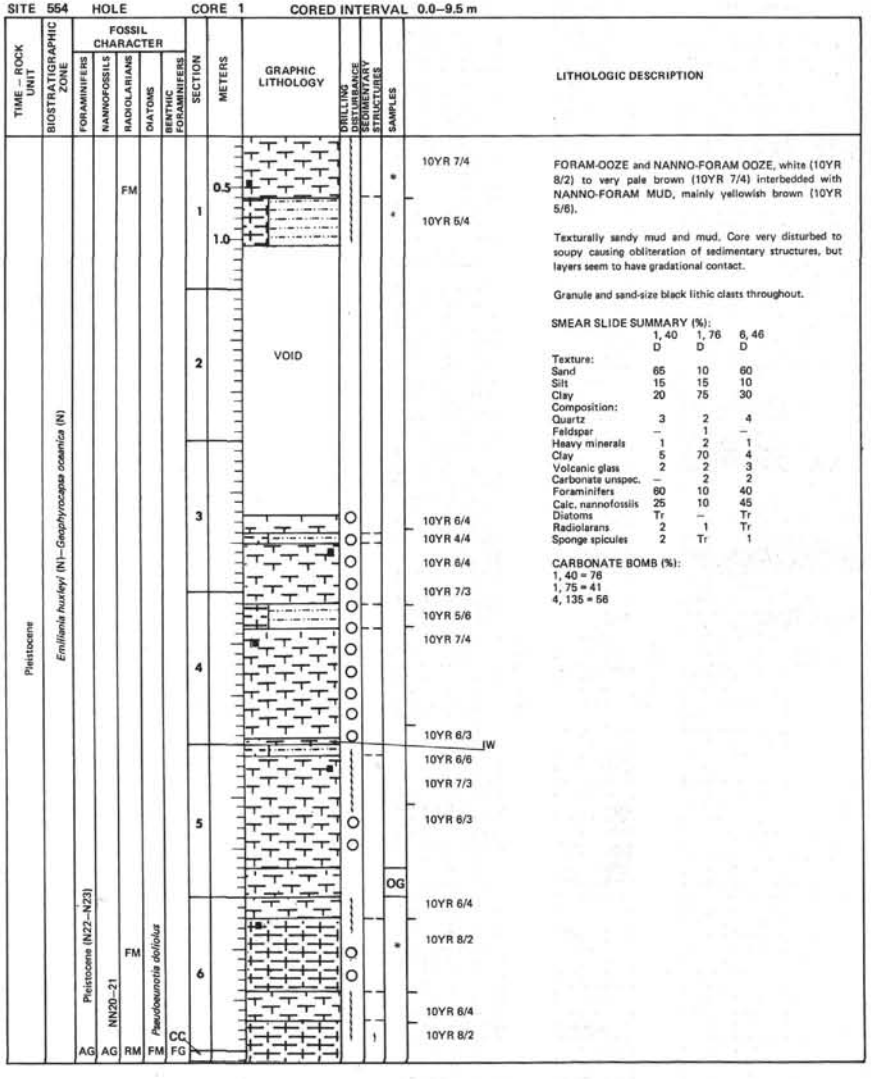

FORAM-OOZE and NANNO-FORAM OOZE, white (10YR 8/2) to very pale brown (10YR 7/4) interbedded with NANNO-FORAM MUD, mainly yellowish brown (10YR 5/6).

Texturally sandy mud and mud. Core very disturbed to soupy causing obliteration of sedimentary structures, but layers seem to have gradational contact.

Granule and sand-size black lithic clasts throughout.

SMEAR SLIDE SUMMARY (%):

	1, 40 D	1, 76 D	6, 46 D
Texture:			
Sand	65	10	60
Silt	15	15	10
Clay	20	75	30
Composition:			
Quartz	3	2	4
Feldspar	–	1	–
Heavy minerals	1	2	1
Clay	5	70	4
Volcanic glass	2	2	3
Carbonate unspec.	–	2	2
Foraminifers	60	10	40
Calc. nannofossils	25	10	45
Diatoms	Tr	–	Tr
Radiolarans	2	1	Tr
Sponge spicules	2	Tr	1

CARBONATE BOMB (%):
1, 40 = 76
1, 75 = 41
4, 135 = 56

SITE 554 HOLE CORE 2 CORED INTERVAL 9.5–19.0 m

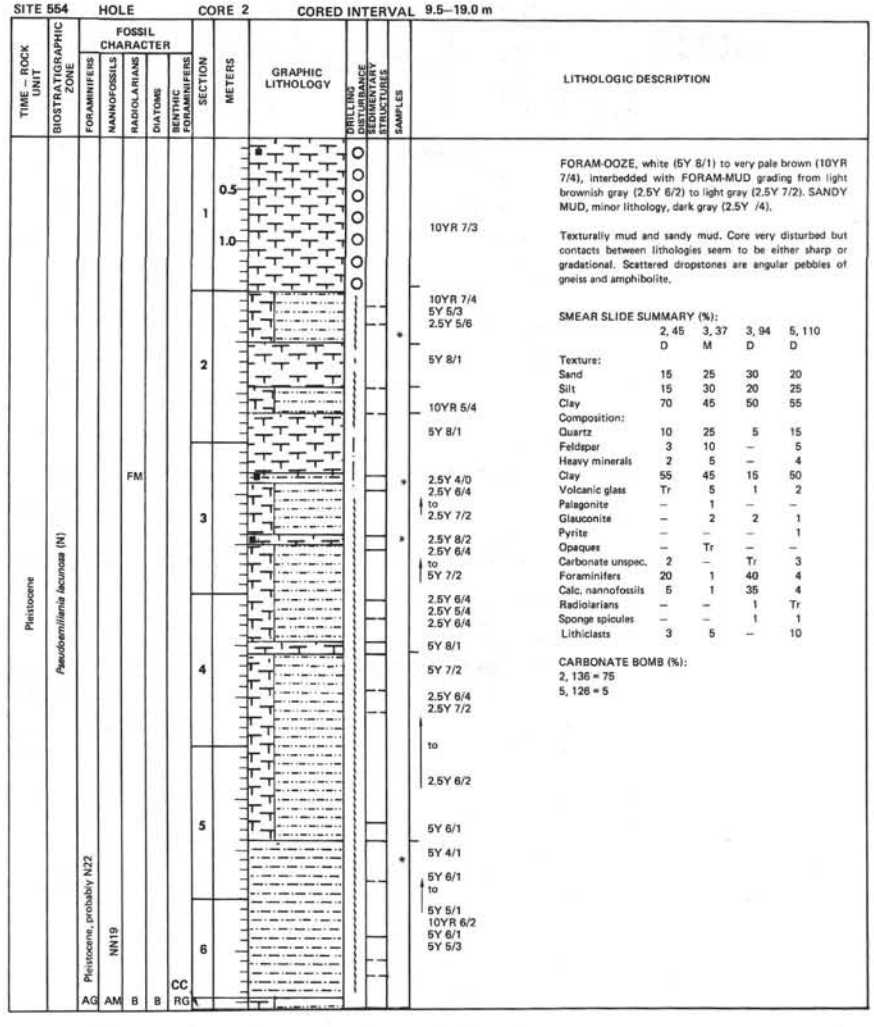

FORAM-OOZE, white (5Y 8/1) to very pale brown (10YR 7/4), interbedded with FORAM-MUD grading from light brownish gray (2.5Y 6/2) to light gray (2.5Y 7/2). SANDY MUD, minor lithology, dark gray (2.5Y /4).

Texturally mud and sandy mud. Core very disturbed but contacts between lithologies seem to be either sharp or gradational. Scattered dropstones are angular pebbles of gneiss and amphibolite.

SMEAR SLIDE SUMMARY (%):

	2, 45 D	3, 37 M	3, 94 D	5, 110 D
Texture:				
Sand	15	25	30	20
Silt	15	30	20	25
Clay	70	45	50	55
Composition:				
Quartz	10	25	5	15
Feldspar	3	10	–	5
Heavy minerals	2	5	–	4
Clay	55	45	15	50
Volcanic glass	Tr	5	1	2
Palagonite	–	1	–	–
Glauconite	–	2	2	1
Pyrite	–	–	–	1
Opaques	–	Tr	–	–
Carbonate unspec.	2	–	Tr	3
Foraminifers	20	1	40	4
Calc. nannofossils	5	1	35	4
Radiolarians	–	–	1	Tr
Sponge spicules	–	–	1	1
Lithiclasts	3	5	–	10

CARBONATE BOMB (%):
2, 136 = 75
5, 126 = 5

SITE 554 HOLE CORE 3 CORED INTERVAL 19.0–28.5 m

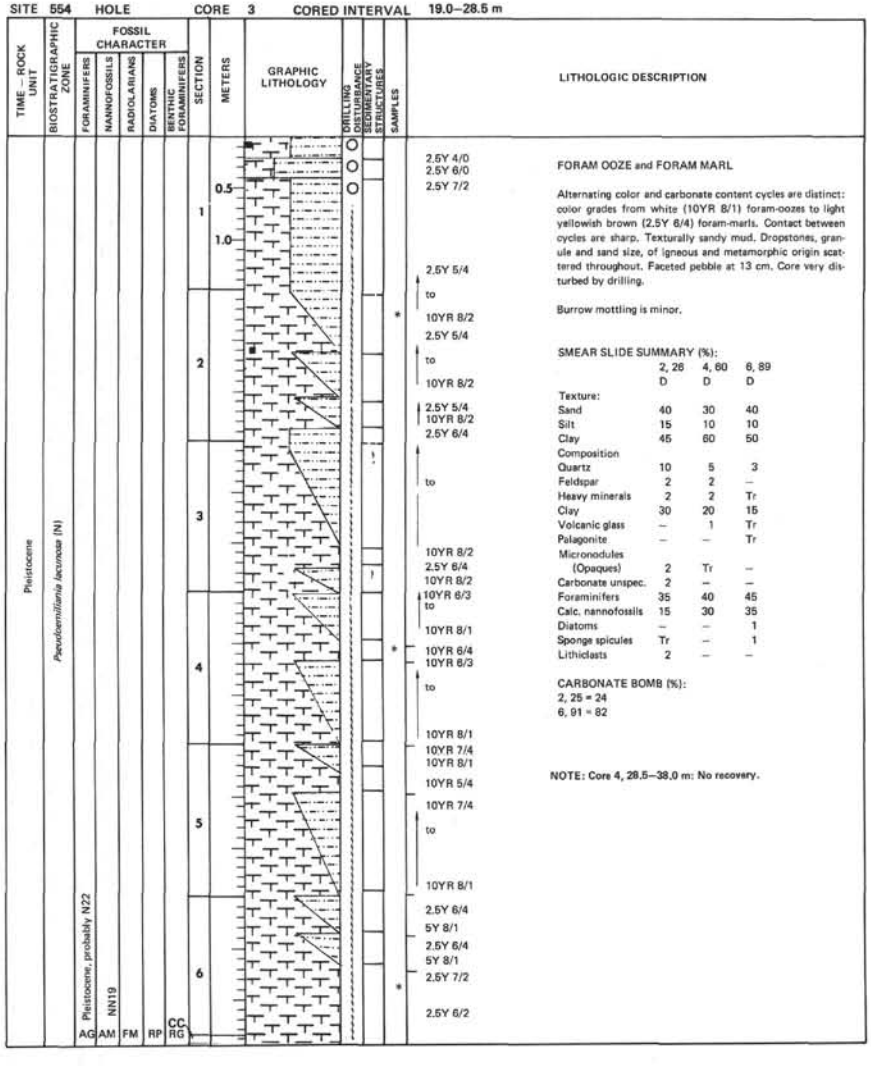

LITHOLOGIC DESCRIPTION

FORAM OOZE and FORAM MARL

Alternating color and carbonate content cycles are distinct: color grades from white (10YR 8/1) foram-oozes to light yellowish brown (2.5Y 6/4) foram-marls. Contact between cycles are sharp. Texturally sandy mud. Dropstones, granule and sand size, of igneous and metamorphic origin scattered throughout. Faceted pebble at 13 cm. Core very disturbed by drilling.

Burrow mottling is minor.

SMEAR SLIDE SUMMARY (%):

	2, 26 D	4, 60 D	6, 89 D
Texture:			
Sand	40	30	40
Silt	15	10	10
Clay	45	60	50
Composition			
Quartz	10	5	3
Feldspar	2	2	–
Heavy minerals	2	2	Tr
Clay	30	20	15
Volcanic glass	–	1	Tr
Palagonite	–	–	Tr
Micronodules (Opaques)	2	Tr	–
Carbonate unspec.	2	–	–
Foraminifers	35	40	45
Calc. nannofossils	15	30	35
Diatoms	–	–	1
Sponge spicules	Tr	–	1
Lithiclasts	2	–	–

CARBONATE BOMB (%):
2, 25 = 24
6, 91 = 82

NOTE: Core 4, 28.5–38.0 m: No recovery.

SITE 554 HOLE CORE 5 CORED INTERVAL 38.0–47.5 m

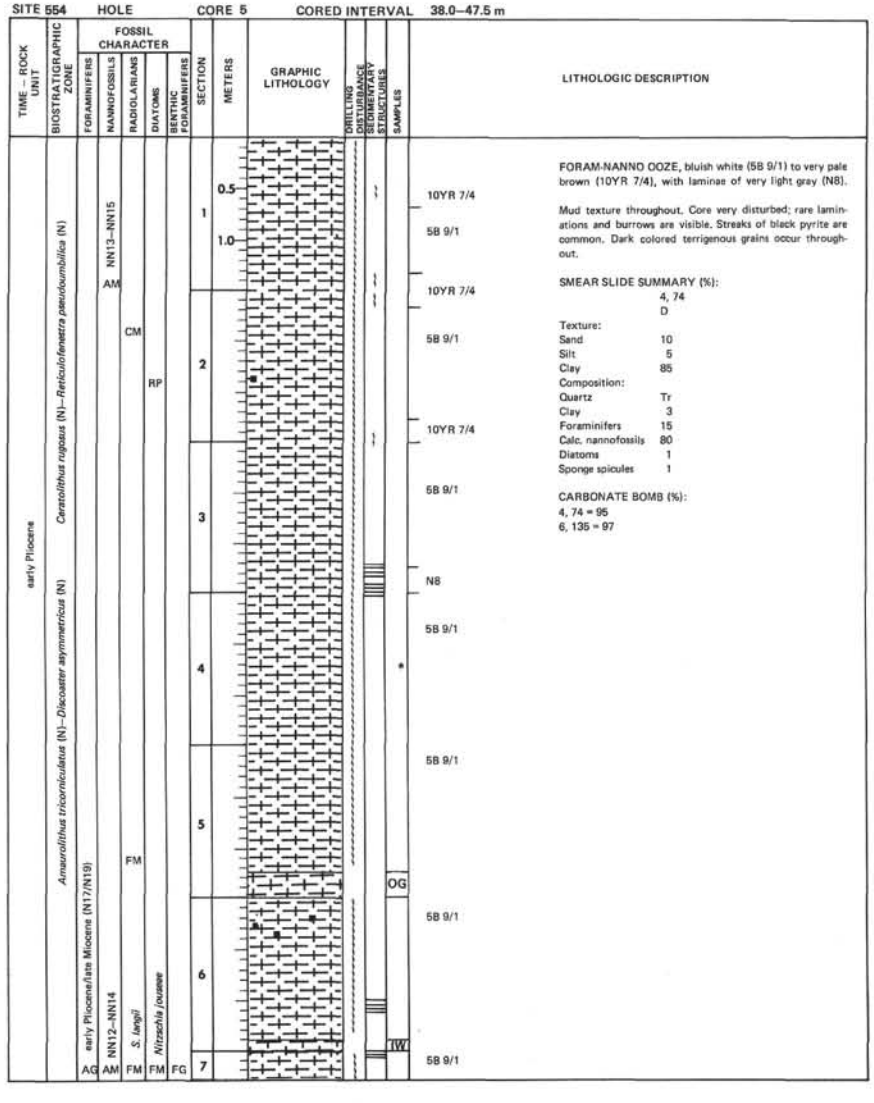

LITHOLOGIC DESCRIPTION

FORAM-NANNO OOZE, bluish white (5B 9/1) to very pale brown (10YR 7/4), with laminae of very light gray (N8).

Mud texture throughout. Core very disturbed; rare laminations and burrows are visible. Streaks of black pyrite are common. Dark colored terrigenous grains occur throughout.

SMEAR SLIDE SUMMARY (%):

	4, 74 D
Texture:	
Sand	10
Silt	5
Clay	85
Composition:	
Quartz	Tr
Clay	3
Foraminifers	15
Calc. nannofossils	80
Diatoms	1
Sponge spicules	1

CARBONATE BOMB (%):
4, 74 = 95
6, 135 = 97

SITE 554 HOLE CORE 6 CORED INTERVAL 47.5–57.0 m

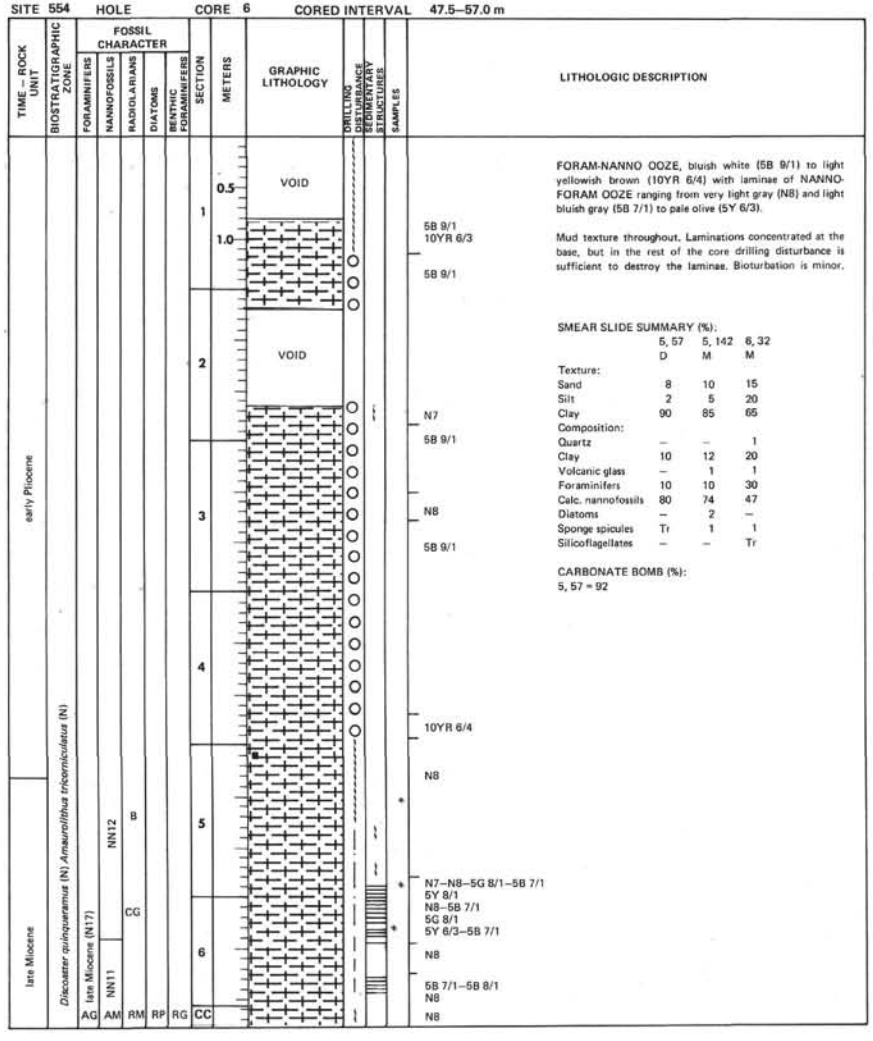

LITHOLOGIC DESCRIPTION

FORAM-NANNO OOZE, bluish white (5B 9/1) to light yellowish brown (10YR 6/4) with laminae of NANNO-FORAM OOZE ranging from very light gray (N8) and light bluish gray (5B 7/1) to pale olive (5Y 6/3).

Mud texture throughout. Laminations concentrated at the base, but in the rest of the core drilling disturbance is sufficient to destroy the laminae. Bioturbation is minor.

SMEAR SLIDE SUMMARY (%):

	5, 57 D	5, 142 M	6, 32 M
Texture:			
Sand	8	10	15
Silt	2	5	20
Clay	90	85	65
Composition:			
Quartz	–	–	1
Clay	10	12	20
Volcanic glass	–	1	1
Foraminifers	10	10	30
Calc. nannofossils	80	74	47
Diatoms	–	2	–
Sponge spicules	Tr	1	1
Silicoflagellates	–	–	Tr

CARBONATE BOMB (%):
5, 57 = 92

SITE 554 HOLE CORE 7 CORED INTERVAL 57.0–66.5 m

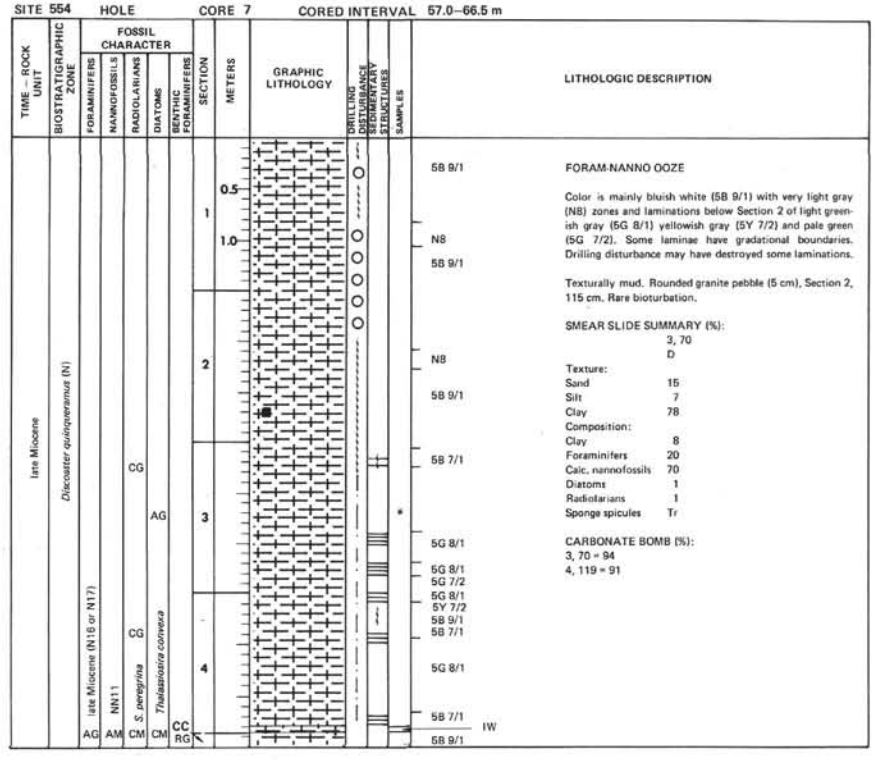

LITHOLOGIC DESCRIPTION

FORAM-NANNO OOZE

Color is mainly bluish white (5B 9/1) with very light gray (N8) zones and laminations below Section 2 of light greenish gray (5G 8/1) yellowish gray (5Y 7/2) and pale green (5G 7/2). Some laminae have gradational boundaries. Drilling disturbance may have destroyed some laminations.

Texturally mud. Rounded granite pebble (5 cm), Section 2, 115 cm. Rare bioturbation.

SMEAR SLIDE SUMMARY (%):

	3, 70 D
Texture:	
Sand	15
Silt	7
Clay	78
Composition:	
Clay	8
Foraminifers	20
Calc. nannofossils	70
Diatoms	1
Radiolarians	1
Sponge spicules	Tr

CARBONATE BOMB (%):
3, 70 = 94
4, 119 = 91

SITE 554 HOLE CORE 8 CORED INTERVAL 66.5–76.0 m

LITHOLOGIC DESCRIPTION

FORAM-NANNO OOZE

Color is mainly bluish white (5B 9/1) with light gray (N7) patches and light greenish gray (5G 8/1) laminae. Patches represent deformed laminae by drilling. Burrow mottling occur in some laminae.

Texturally mud. Granule and sand-size dropstones of metamorphic origin in Sections 1–2.

SMEAR SLIDE SUMMARY (%):

	4, 70 D
Texture:	
Sand	15
Silt	5
Clay	80
Composition:	
Clay	10
Foraminifers	20
Calc. nannofossils	70
Diatoms	Tr
Radiolarians	Tr
Sponge spicules	Tr

CARBONATE BOMB (%):
4, 70 = 93

SITE 554 HOLE A CORE 1 CORED INTERVAL 76.0–85.5 m

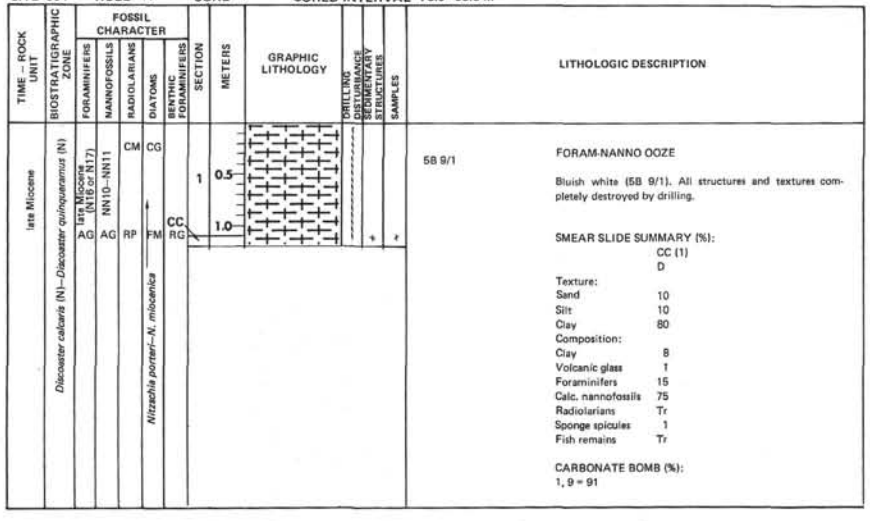

LITHOLOGIC DESCRIPTION

FORAM-NANNO OOZE

Bluish white (5B 9/1). All structures and textures completely destroyed by drilling.

SMEAR SLIDE SUMMARY (%):

	CC (1) D
Texture:	
Sand	10
Silt	10
Clay	80
Composition:	
Clay	8
Volcanic glass	1
Foraminifers	15
Calc. nannofossils	75
Radiolarians	Tr
Sponge spicules	1
Fish remains	Tr

CARBONATE BOMB (%):
1, 9 = 91

SITE 554 HOLE A CORE 2 CORED INTERVAL 85.5–95.0 m

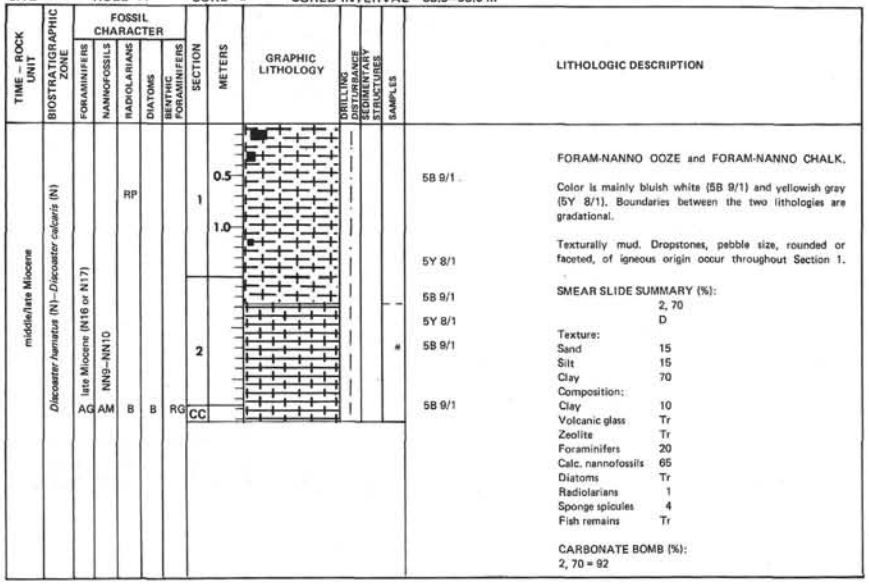

LITHOLOGIC DESCRIPTION

FORAM-NANNO OOZE and FORAM-NANNO CHALK.

Color is mainly bluish white (5B 9/1) and yellowish gray (5Y 8/1). Boundaries between the two lithologies are gradational.

Texturally mud. Dropstones, pebble size, rounded or faceted, of igneous origin occur throughout Section 1.

SMEAR SLIDE SUMMARY (%):

	2, 70 D
Texture:	
Sand	15
Silt	15
Clay	70
Composition:	
Clay	10
Volcanic glass	Tr
Zeolite	Tr
Foraminifers	20
Calc. nannofossils	65
Diatoms	Tr
Radiolarians	1
Sponge spicules	4
Fish remains	Tr

CARBONATE BOMB (%):
2, 70 = 92

SITE 554 HOLE A CORE 3 CORED INTERVAL 95.0–104.5 m

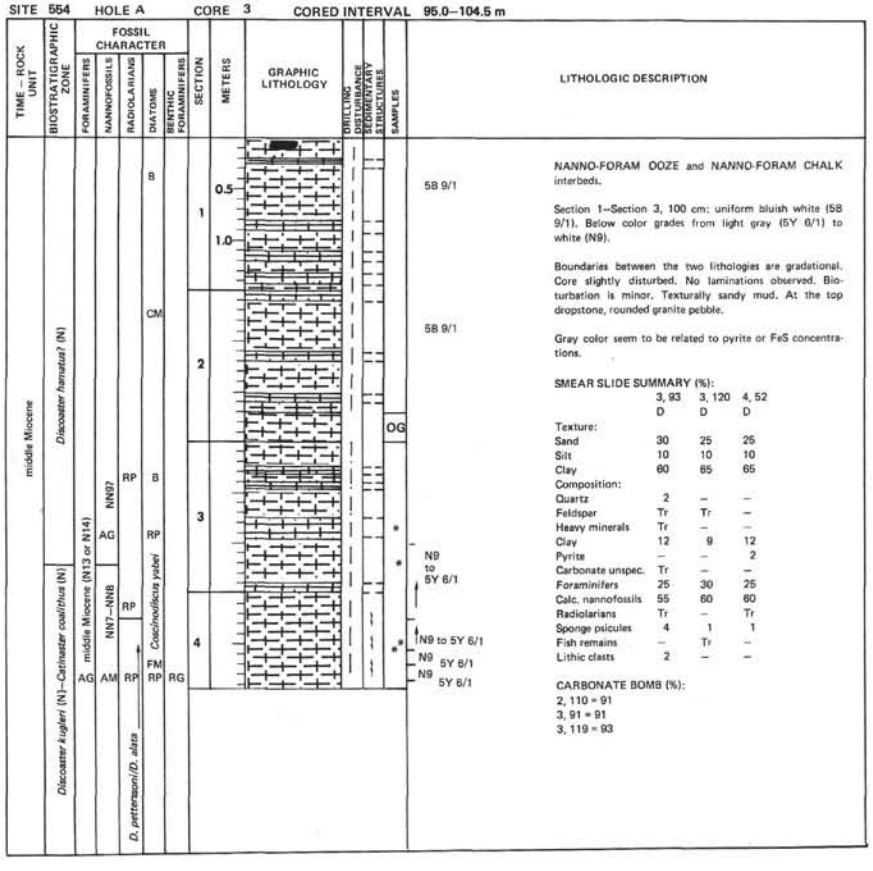

LITHOLOGIC DESCRIPTION

NANNO-FORAM OOZE and NANNO-FORAM CHALK interbeds.

Section 1–Section 3, 100 cm: uniform bluish white (5B 9/1). Below color grades from light gray (5Y 6/1) to white (N9).

Boundaries between the two lithologies are gradational. Core slightly disturbed. No laminations observed. Bioturbation is minor. Texturally sandy mud. At the top dropstone, rounded granite pebble.

Gray color seem to be related to pyrite or FeS concentrations.

SMEAR SLIDE SUMMARY (%):

	3, 93 D	3, 120 D	4, 52 D
Texture:			
Sand	30	25	25
Silt	10	10	10
Clay	60	65	65
Composition:			
Quartz	2	–	–
Feldspar	Tr	Tr	–
Heavy minerals	Tr	–	–
Clay	12	9	12
Pyrite	–	–	2
Carbonate unspec.	Tr	–	–
Foraminifers	25	30	25
Calc. nannofossils	55	60	60
Radiolarians	Tr	–	Tr
Sponge psicules	4	1	1
Fish remains	–	Tr	–
Lithic clasts	2	–	–

CARBONATE BOMB (%):
2, 110 = 91
3, 91 = 91
3, 119 = 93

SITE 554 HOLE A CORE 4 CORED INTERVAL 104.5–114.0 m

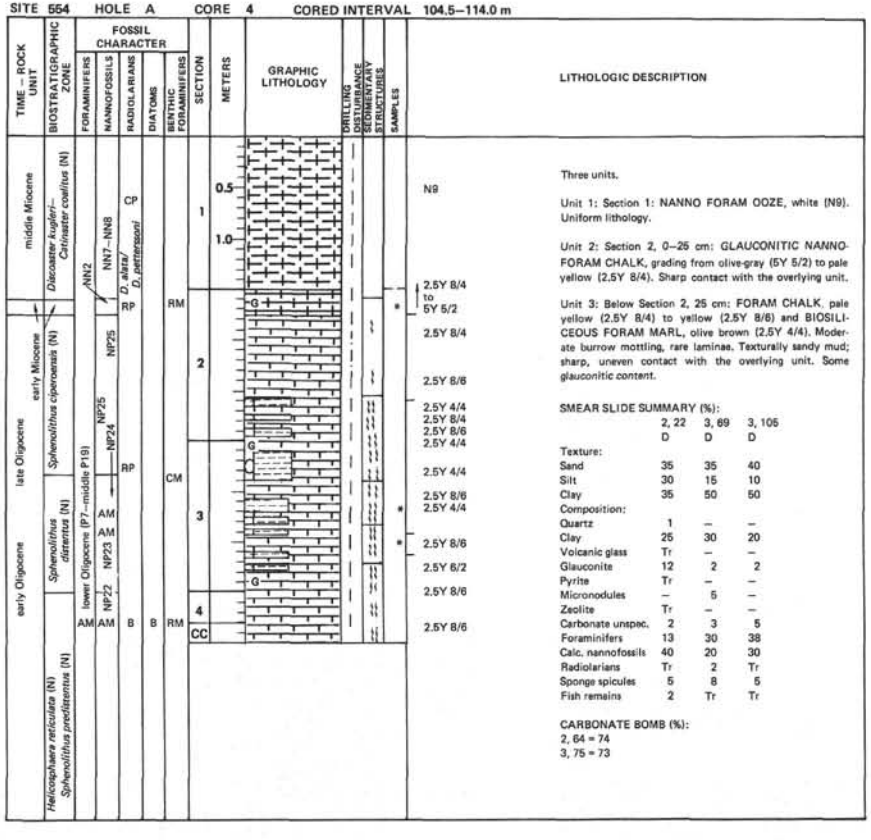

LITHOLOGIC DESCRIPTION

Three units.

Unit 1: Section 1: NANNO FORAM OOZE, white (N9). Uniform lithology.

Unit 2: Section 2, 0–25 cm: GLAUCONITIC NANNO-FORAM CHALK, grading from olive-gray (5Y 5/2) to pale yellow (2.5Y 8/4). Sharp contact with the overlying unit.

Unit 3: Below Section 2, 25 cm: FORAM CHALK, pale yellow (2.5Y 8/4) to yellow (2.5Y 8/6) and BIOSILICEOUS FORAM MARL, olive brown (2.5Y 4/4). Moderate burrow mottling, rare laminae. Texturally sandy mud; sharp, uneven contact with the overlying unit. Some *glauconitic content*.

SMEAR SLIDE SUMMARY (%):

	2, 22 D	3, 69 D	3, 105 D
Texture:			
Sand	35	35	40
Silt	30	15	10
Clay	35	50	50
Composition:			
Quartz	1	–	–
Clay	25	30	20
Volcanic glass	Tr	–	–
Glauconite	12	2	2
Pyrite	Tr	–	–
Micronodules	–	5	–
Zeolite	Tr	–	–
Carbonate unspec.	2	3	5
Foraminifers	13	30	38
Calc. nannofossils	40	20	30
Radiolarians	Tr	2	Tr
Sponge spicules	5	8	5
Fish remains	2	Tr	Tr

CARBONATE BOMB (%):
2, 64 = 74
3, 75 = 73

SITE 554 HOLE A CORE 5 CORED INTERVAL 114.0–123.5 m

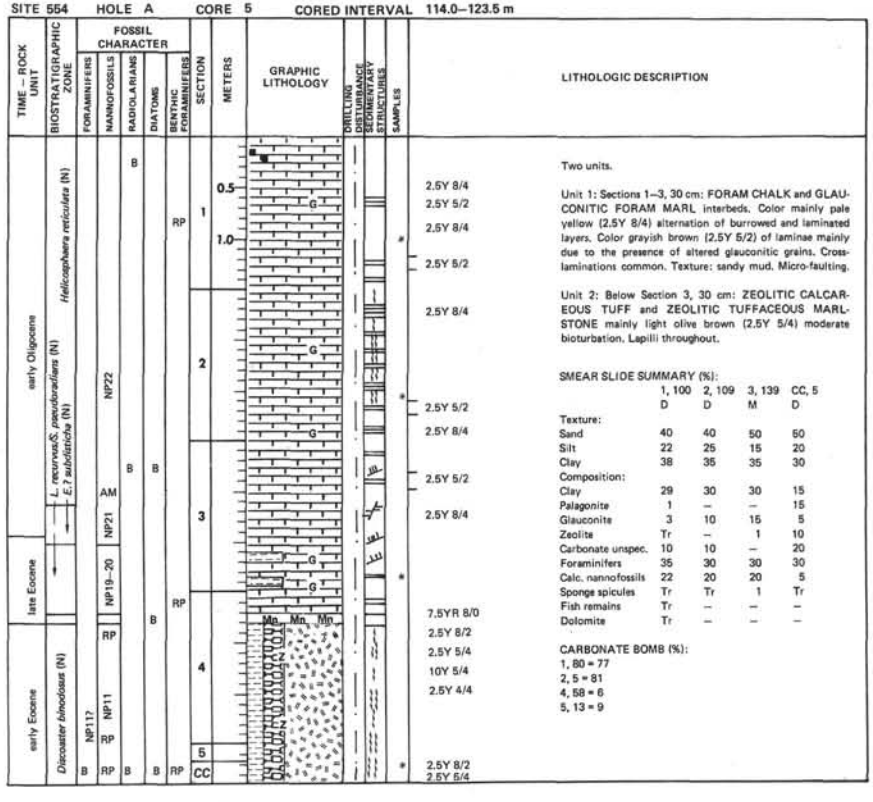

LITHOLOGIC DESCRIPTION

Two units.

Unit 1: Sections 1–3, 30 cm: FORAM CHALK and GLAUCONITIC FORAM MARL interbeds. Color mainly pale yellow (2.5Y 8/4) alternation of burrowed and laminated layers. Color grayish brown (2.5Y 5/2) of laminae mainly due to the presence of altered glauconitic grains. Cross-laminations common. Texture: sandy mud. Micro-faulting.

Unit 2: Below Section 3, 30 cm: ZEOLITIC CALCAREOUS TUFF and ZEOLITIC TUFFACEOUS MARLSTONE mainly light olive brown (2.5Y 5/4) moderate bioturbation. Lapilli throughout.

SMEAR SLIDE SUMMARY (%):

	1, 100 D	2, 109 D	3, 139 M	CC, 5 D
Texture:				
Sand	40	40	50	50
Silt	22	25	15	20
Clay	38	35	35	30
Composition:				
Clay	29	30	30	15
Palagonite	1	–	–	15
Glauconite	3	10	15	5
Zeolite	Tr	–	1	10
Carbonate unspec.	10	10	–	20
Foraminifers	35	30	30	30
Calc. nannofossils	22	20	20	5
Sponge spicules	Tr	Tr	1	Tr
Fish remains	Tr	–	–	–
Dolomite	Tr	–	–	–

CARBONATE BOMB (%):
1, 80 = 77
2, 5 = 81
4, 58 = 6
5, 13 = 9

SITE 554 HOLE A CORE 6 CORED INTERVAL 123.5–133.0 m

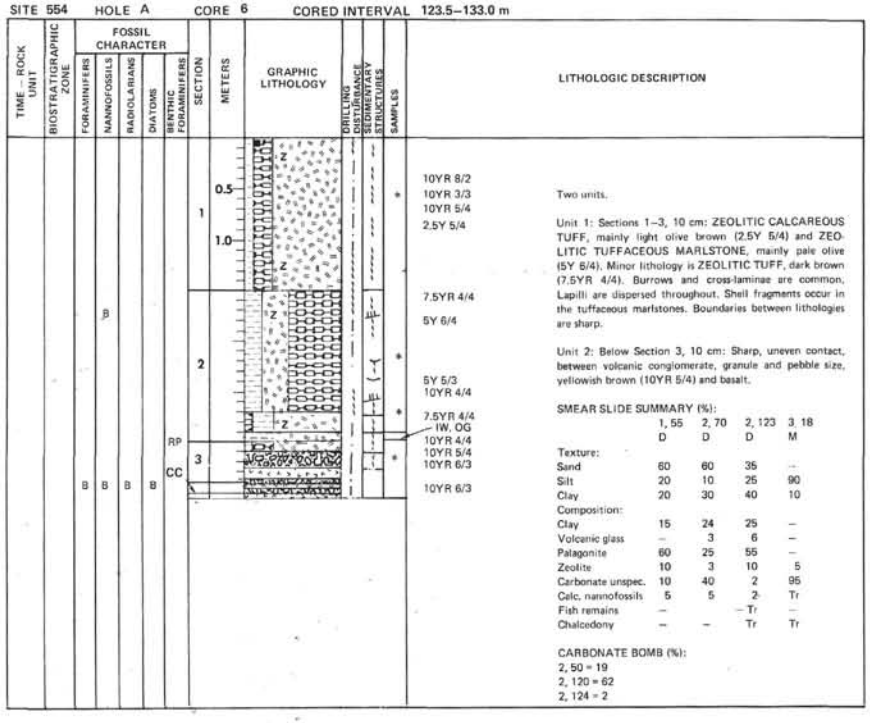

LITHOLOGIC DESCRIPTION

Two units.

Unit 1: Sections 1–3, 10 cm: ZEOLITIC CALCAREOUS TUFF, mainly light olive brown (2.5Y 5/4) and ZEOLITIC TUFFACEOUS MARLSTONE, mainly pale olive (5Y 6/4). Minor lithology is ZEOLITIC TUFF, dark brown (7.5YR 4/4). Burrows and cross-laminae are common. Lapilli are dispersed throughout. Shell fragments occur in the tuffaceous marlstones. Boundaries between lithologies are sharp.

Unit 2: Below Section 3, 10 cm: Sharp, uneven contact, between volcanic conglomerate, granule and pebble size, yellowish brown (10YR 5/4) and basalt.

SMEAR SLIDE SUMMARY (%):

	1, 55 D	2, 70 D	2, 123 D	3, 18 M
Texture:				
Sand	60	60	35	–
Silt	20	10	25	90
Clay	20	30	40	10
Composition:				
Clay	15	24	25	–
Volcanic glass	–	3	6	–
Palagonite	60	25	55	–
Zeolite	10	3	10	5
Carbonate unspec.	10	40	2	95
Calc. nannofossils	5	5	2	Tr
Fish remains	–		Tr	–
Chalcedony	–	–	Tr	Tr

CARBONATE BOMB (%):
2, 50 = 19
2, 120 = 62
2, 124 = 2

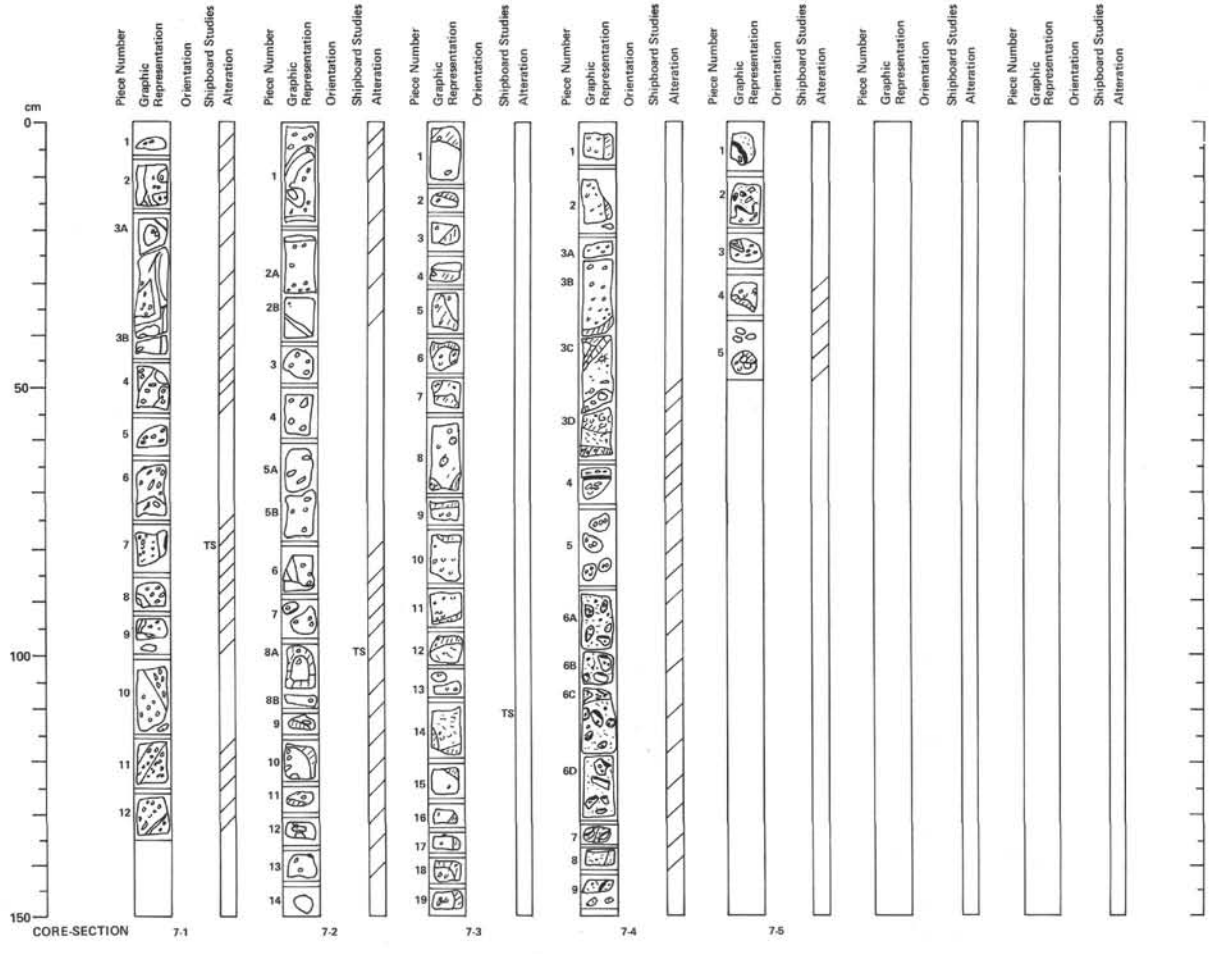

CORE 7, SECTION 1 Depth 133–134.5 m

This section is vesicular basalt and moderately altered (palagonite and calcite common).

Piece 1: Vesicular (~0.5–1 mm, empty), aphyric gray (10YR 5/1) basalt.

Piece 2: Irregular vein (2 mm) infilled with calcite and black mineral. Weathered vein (1 cm) on fresh basalt. Vesicular (1 mm) unevenly distributed. Brecciated and cemented with calcite. Clasts of palagonite (1–5 mm).

Piece 3: Fractured basalt (aphyric) – fresh rounded much with alteration vein (1 cm thick) related to fractures (calcite filled – 1 mm and black mineral). Vesicles irregular distribution (0.5–2 mm – some lined with green clay and few filled with calcite) pale brown (10YR 6/3) (alteration color). Micritic (recrystallized marl?) incorporated as clast pale yellow (5Y 8/4).

Pieces 5, 8, and 7: Relatively fresh aphyric basalt – scattered (0.5–4 mm) vesicles with vertical elongation, mostly empty, some with clay and spar calcite. Piece 7 has yellow (2.5Y 8/8) sediment inclusion (calcareous).

Pieces 8–12: Fresh vesicular basalt and veins infilled with marl with 1 cm alteration margins. One cm fracture with calcite spar partly filling fresh basalt. Vertically zoned vesicles some filled with calcite. Fresh vesicular basalt, with irregular fracture filled with muddy calcite and spar. Two percent of vesicles filled with clear calcite.

CORE 7, SECTION 2 Depth 134.5–136.0 m

Pieces 1 and 2: Aphyric basalt gray (2.5Y 6/0), vesicles irregular distribution (1 mm–4 mm) most empty, irregular shape and elongated. Fractures: 1 mm, clear calcite with 2 cm alteration zone into basalt. Lithified inclusions of yellow chalk with palagonite clasts – may be a soft sediment clast (or angular). Piece 2B has a 5 mm vein filled with sediment (sand size palagonite and basalt grains). Some vesicles filled with clear calcite and some lined with green clay.

Pieces 3–5: Irregular, scattered vesicles up to 15 cm. Most empty. Fewer vesicles at base.

Pieces 6–14: Few vesicles (up to 5 mm), alteration veins (1 cm) around some pieces bounded by fractures. Fractures filled by calcite and others by very fine-grained chalky calcite.

CORE 7, SECTION 3 Depth 136.0–137.5 m

Relatively fresh basalt with few vesicles. Some filled with black mineral. The aphyric basalt fragments contain inclusions of very vesicular phase (2–3 cm). This pumice has altered to zeolites and clay. Color is gray (2.5Y 6/0). Some pieces are bounded by fractures which have an alteration zone into the basalt. Light gray basalt has vein of darker gray alteration.

Pieces 12–14: Contain sub-horizontal streaks of darker color.

CORE 7, SECTION 4 Depth 137.5–139.0 m

Pieces 1–3B: Aphyric basalt with scattered vesicles (1–2 mm). Most vesicles are empty.

Piece 3C: Altered basalt at base of flow unit.

Pieces 3C and D: Angular fragments of basalt and devitrified glass (1 mm to 2 cm in size) cemented by white (fine grained calcite). Hyaloclastite?

Piece 4: Base of flow with palagonite rim (greenish gray [5G 6/1], dark brown [7.5YR 4/4]). Some fragmented vesicular basalt infilled with calcite.

Pieces 4–9: Conglomerate, matrix supported with some original voids now filled with calcite spar (one geopetal structure in a void). Pebbles are both angular and rounded and consist of basalt (sometimes with palagonite rim or partial rim), palagonite clasts and vesicular basalt clasts. Matrix sand is altered glass and basalt grains cemented by calcite. Some calcite veins and as partial filling of voids. Piece 8 has weakly developed bedding and size sorting.

CORE 7, SECTION 5 Depth 139.0–139.5 m

Pieces 1–3: Conglomerate of basalt pebbles (angular) and some rounded palagonite pebbles in calcite cemented matrix of basaltic sand grains (as previous section).

Pieces 4 and 5: Basalt (aphyric) with few vesicles – some empty and others up to 1 cm filled with calcite.

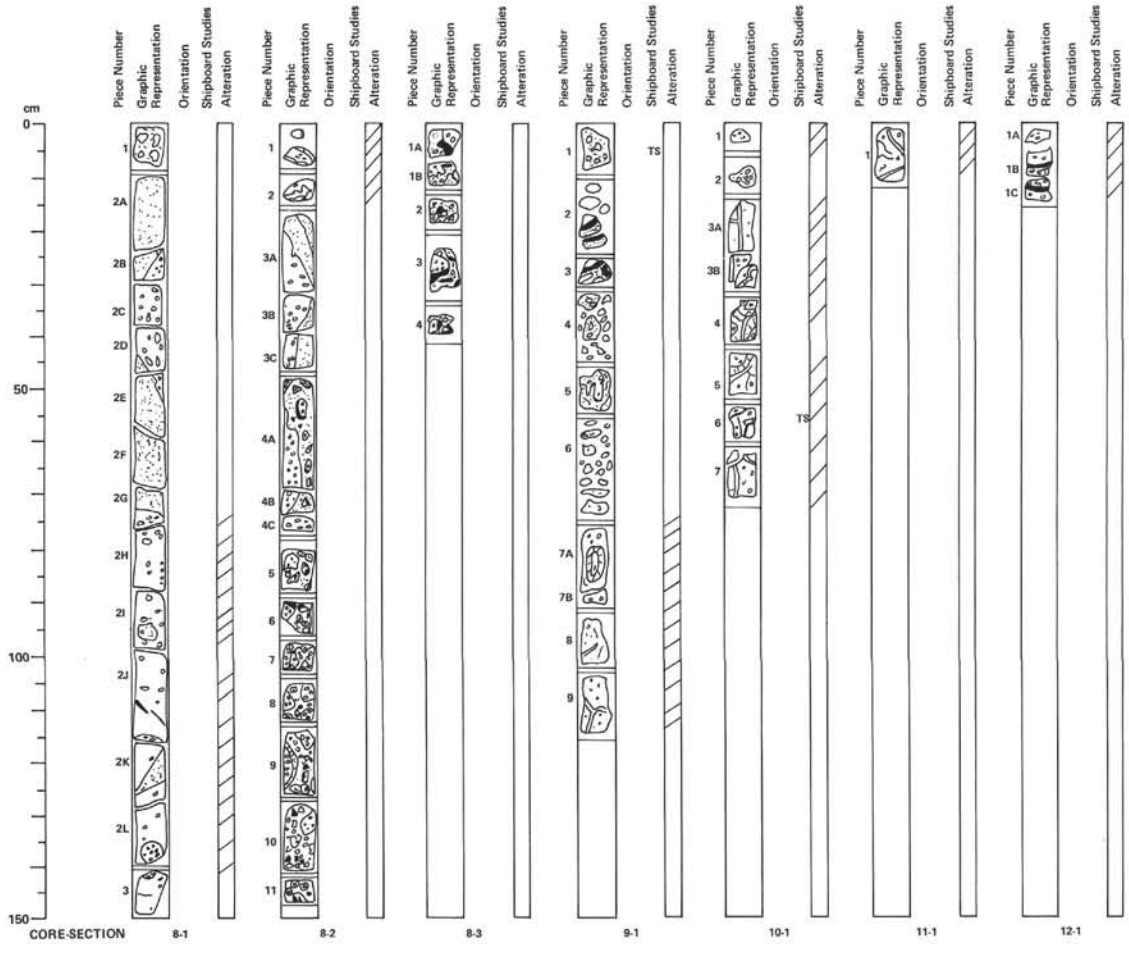

CORE 8, SECTION 1 Depth 142.5–144.0 m

Piece 1: Clast supported conglomerate with calcite cemented sand matrix. Clasts are 0.5–1 cm in size, angular to sub-rounded. Composed of basalt and weathered basalt and palagonite. Sand matrix is palagonite and basalt and subrounded.

Piece 2A: Volcaniclastic sandstone. Well sorted, no matrix, subangular to rounded, composed of basalt and glass. Calcite cemented.

Pieces 2B and C: Inclined contact between sandstone and basalt pinkish gray (7.5YR 6/2). Basalt is vesicular (1 cm elongated vertical), some are empty, others are infilled with calcite. This basalt may be boulder in the sandstone.

Pieces 2D and E: Inclined contact with underlying sandstone.

Piece 2F: Volcaniclastic sandstone as above with bedding reflecting grain size (up to granule size).

Piece 2G: Inclined contact with underlying basalt (as above).

Piece 2H: Vesicles (0.5–1 cm) becoming rare with depth.

Piece 2I: Some very vesicular inclusions (3–4 cm) in the basalt.

Piece 2J: Vein of calcite, irregular.

Piece 2K: Wedge of volcaniclastic sandstone filling a fracture in the basalt. Calcite cemented. Calcite veins.

Pieces 2L and 3: Altered basalt with inclusions (2–5 cm) that are very similar (pumice – some vesicles filled with yellow [10YR 7/8] and green smectite).

CORE 8, SECTION 2 Depth 144.0–145.5 m

Pieces 1 and 2: Altered basalt as in previous section with inclusions of very vesicular basalt. Irregular vein and vesicles filled with calcite and zeolite.

Piece 3: Volcaniclastic sandstone. Well-sorted, sub-angular to rounded clasts of basalt, altered glass and palagonite. Calcite cemented. Very coarse sand with granules. Inclined (steep) contact with basalt (may be boulder in the sandstone).

Piece 4: Matrix supported conglomerate. Matrix of coarse sand (as sandstone above) and clasts of pebble and boulder size. Some pebbles are basaltic and others are basalt with a palagonite vein (or partial rims). Angular to subrounded pebbles. Calcite cemented filling voids between pebbles. Poorly sorted.

Pieces 5–11: Clast supported conglomerate with no matrix. Cemented by calcite. Pebbles similar to conglomerate above. Some rads only partially filled with calcite. Bimodal pebble size (0.5–1 cm and 2–5 cm). Shape of pebbles very angular to rounded. Indented shape of some pebbles due to vesicles.

CORE 8, SECTION 3 Depth 145.5–145.9 m

Same as conglomerate in Section 2.

CORE 9, SECTION 1 Depth 152.0–153.2 m

Piece 1: Matrix supported conglomerate. Matrix of coarse sand (glass and basaltic fragments) – clasts, palagonitized, altered, pebbles or granules, are baseltic. Angular to subrounded sand and pebble. Calcite cemented, infilling voids between pebbles.

Piece 2: 3 pieces of altered basalt, as in previous core (pinkish gray – 7.5YR 6/2), – 2 pieces of the same altered basalt with palagonite rim (greenish – 5G 6/1 and dark brown – 7.5YR 4/4).

Pieces 3–6: Conglomerate – angular basaltic rock fragments, pebble size, same with palagonite rim, in a sandy matrix. Sand made of glass or basaltic fragments, rounded or sub-angular, calcite cemented.

Pieces 7–9: Altered basalt as above. Fractures filled with calcite. A few very small vesicles.

CORE 10, SECTION 1 Depth 161.5–162.2 m

Piece 1: Basalt. No vesicles.

Piece 2: Conglomerate. No matrix. Clast supported. Cement of calcite, zeolite with porosity. Rounded altered granule pebbles (2–7 mm) of palagonite and basalt.

Pieces 3–7: Altered basalt. Very few vesicles (similar to Core 9, Section 1). In Pieces 6 – fresher basalt with altered rim. Fractures (vertical and horizontal, 2 mm wide) and irregular openings filled with calcite. Alteration margin follows the fractures.

CORE 11, SECTION 1 Depth 171.0–171.1 m

Altered aphyric basalt. Similar to Core 10, Section 1. Irregular fractures filled with calcite (0.5 mm). No vesicles.

CORE 12, SECTION 1 Depth 180.5–180.7 m

Piece 1: Aphyric basalt – no vesicles (similar to core 11, Section 1).

Pieces 1B and C: Palagonite rim (5 mm) with hyaloclastite rim of fragmented palagonite (calcite and zeolite cement with a lot of open pores) on altered basalt.

CORE 13, SECTION 1 Depth 190.0–190.1 m

Altered aphyric basalt as in previous core (Core 12, Section 1) with fractures filled with calcite and black mineral (smectite).

CORE 14, SECTION 1 Depth 199.5–200.5 m

Piece 1: Partly altered grading into fresher aphyric basalt. Very few vesicles (small and empty). Fractured and filled with calcite.

Pieces 2–9: Relatively fresh aphyric basalt. Vesicles are rare. Irregular fractures are common and are filled with green smectite(?) and calcite. Alteration rims in the basalt follow the fractures.

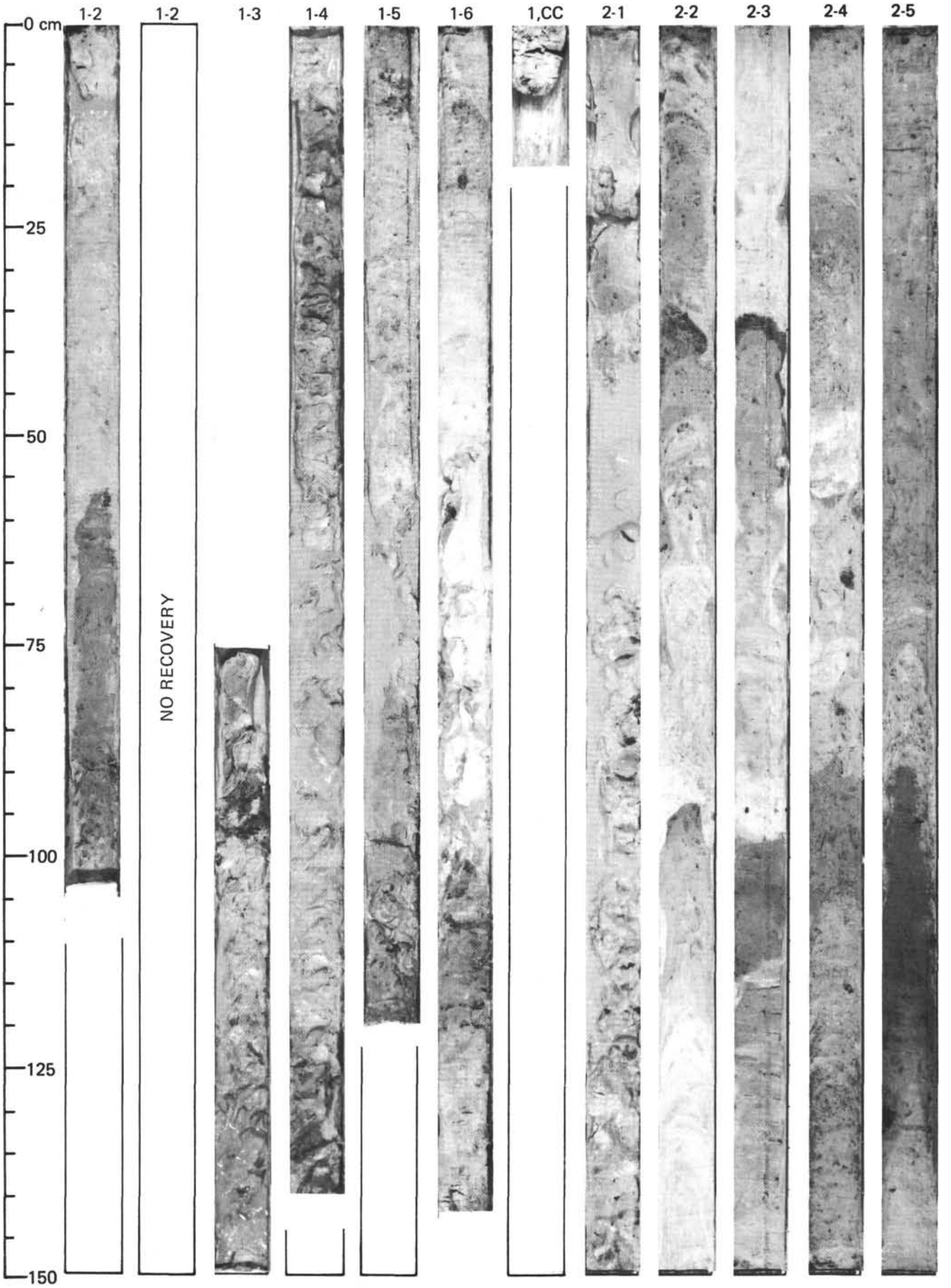
1-2
1-2
1-3
1-4
1-5
1-6
1,CC
2-1
2-2
2-3
2-4
2-5
0 cm
25
50
75
100
125
150
NO RECOVERY

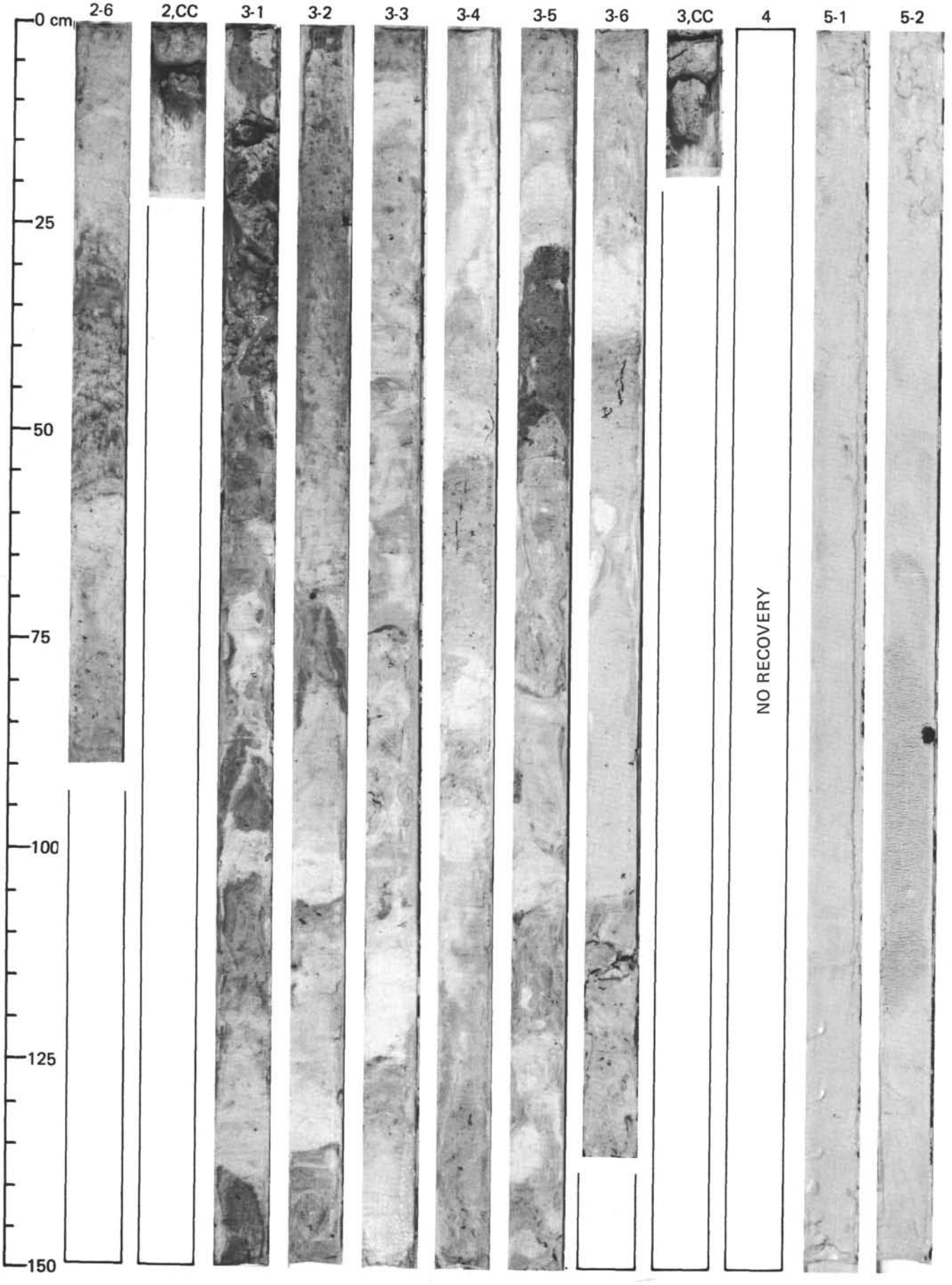
0 cm
25
50
75
100
125
150
2-6
2,CC
3-1
3-2
3-3
3-4
3-5
3-6
3,CC
4
5-1
5-2
NO RECOVERY

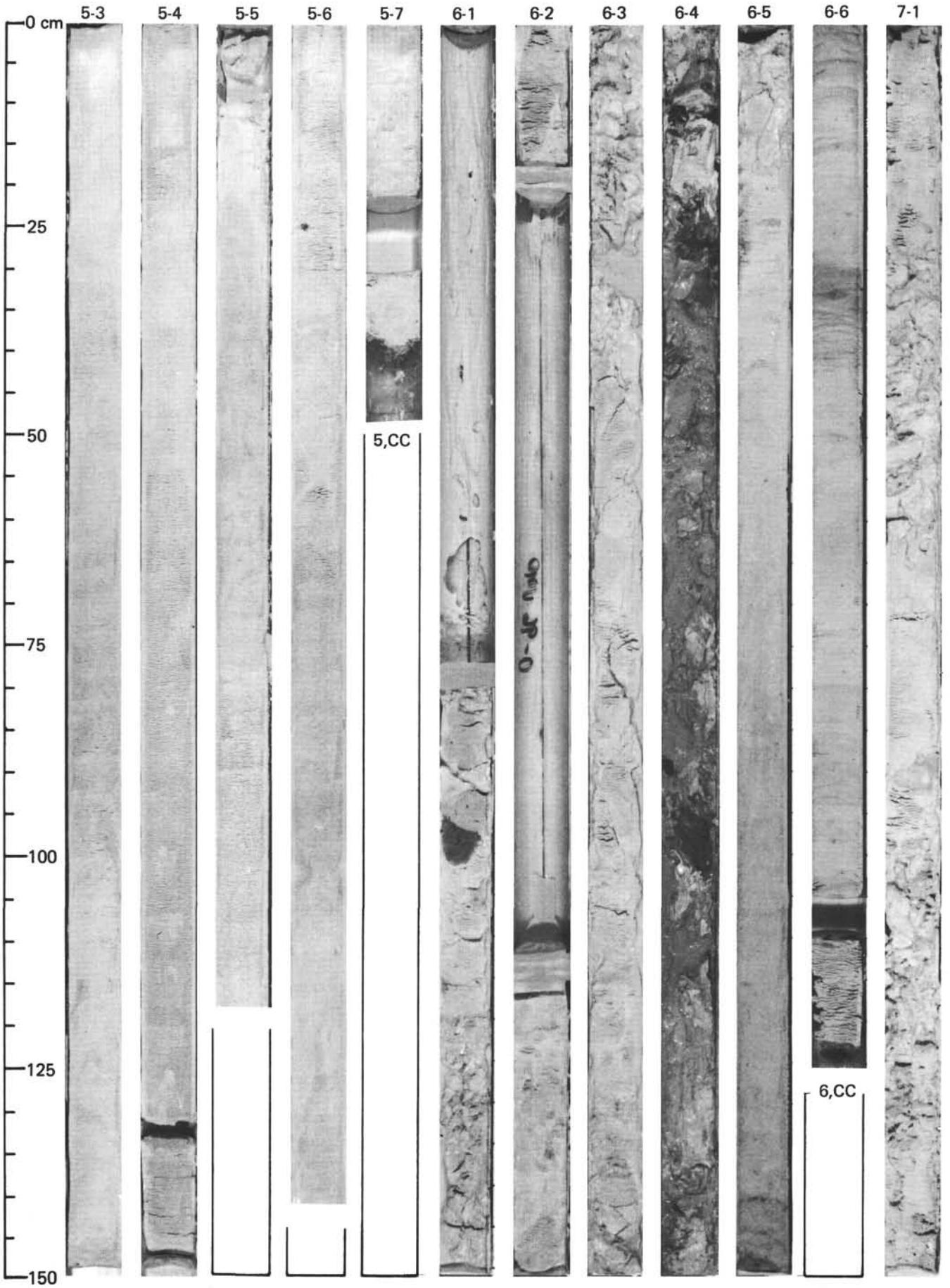
5-3
5-4
5-5
5-6
5-7
6-1
6-2
6-3
6-4
6-5
6-6
7-1
0 cm
25
50
75
100
125
150
5,CC
6,CC

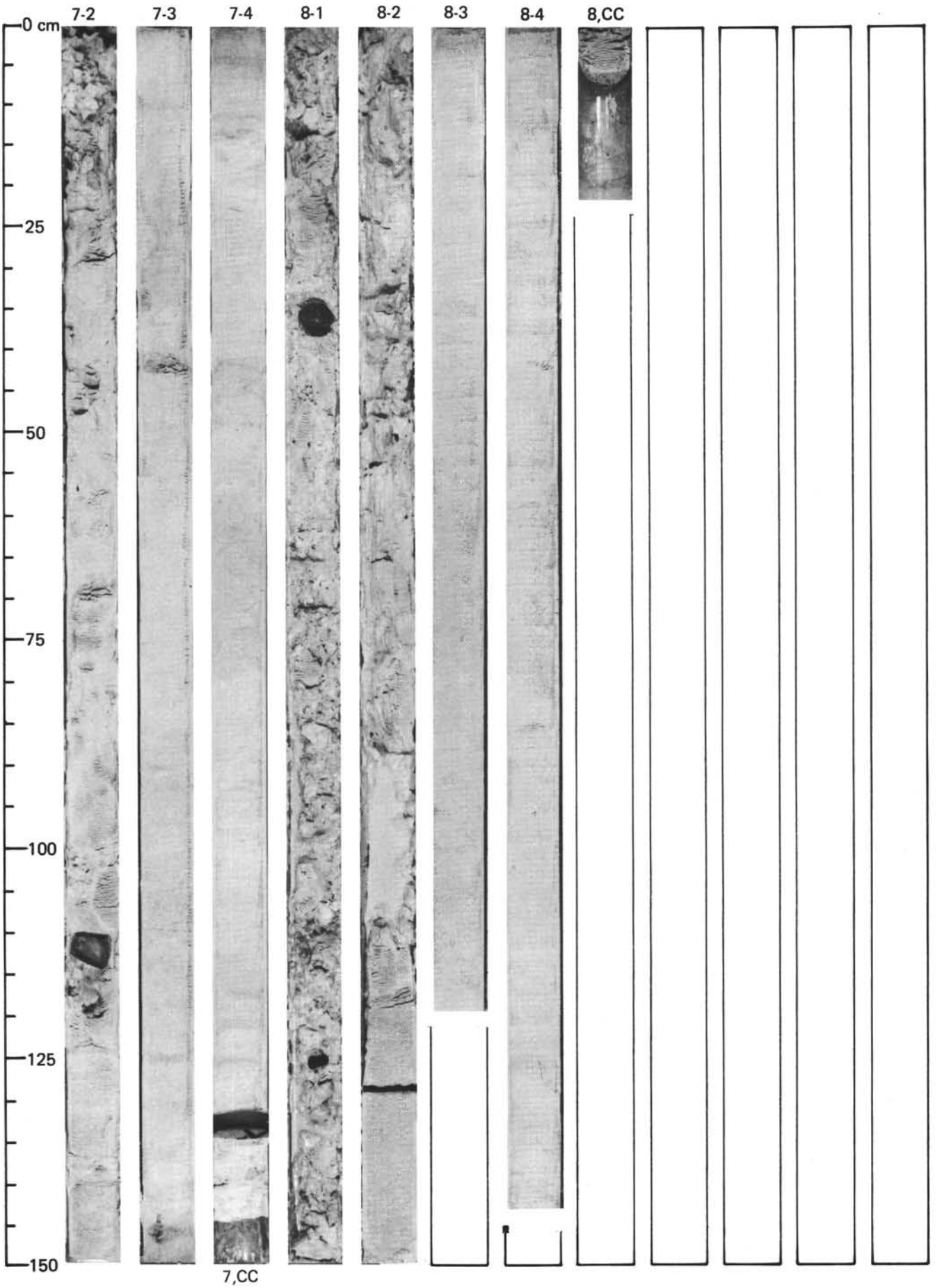
0 cm
25
50
75
100
125
150
7-2
7-3
7-4
8-1
8-2
8-3
8-4
8,CC
7,CC

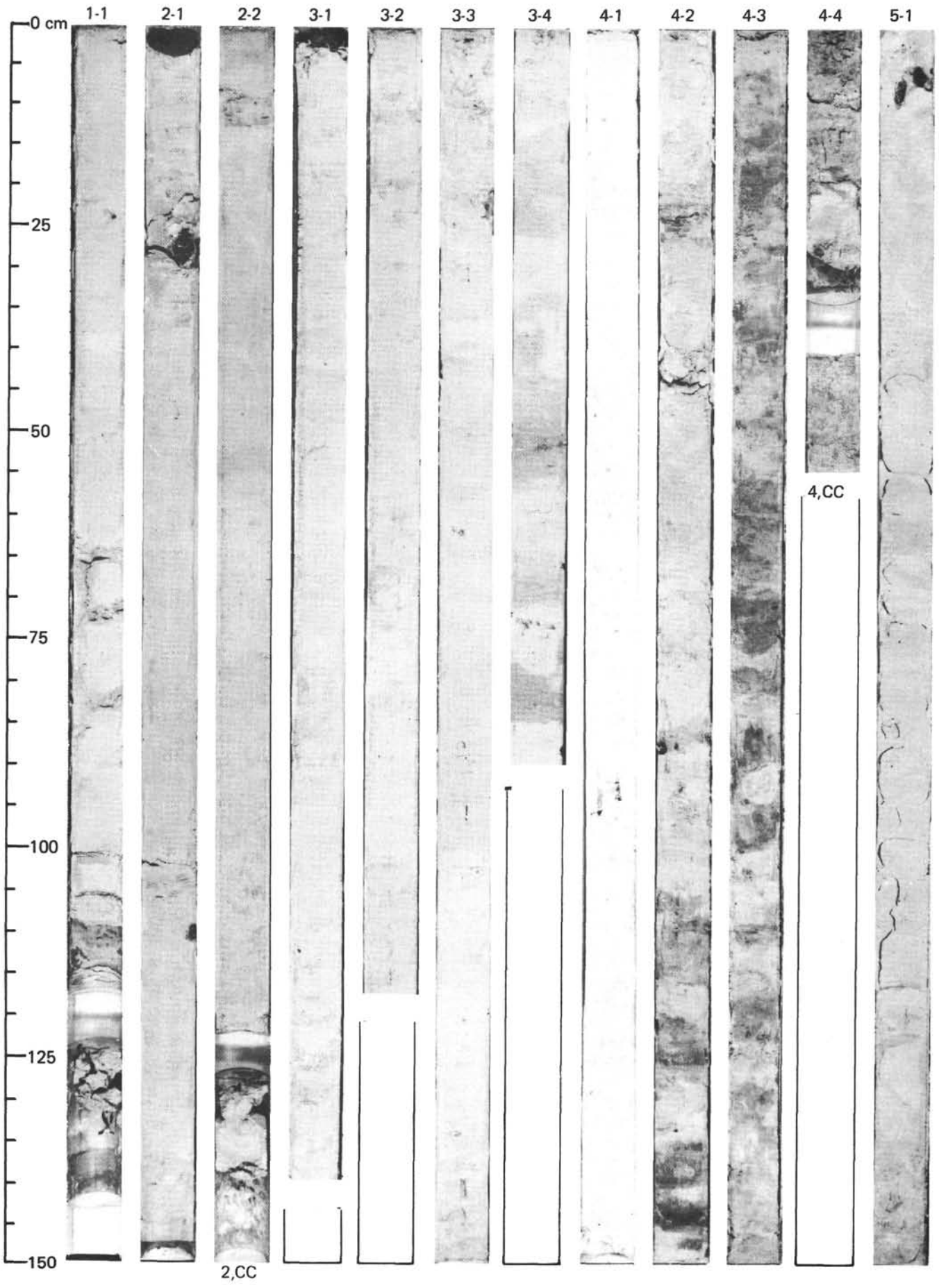
1-1
2-1
2-2
3-1
3-2
3-3
3-4
4-1
4-2
4-3
4-4
5-1
0 cm
25
50
75
100
125
150
2,CC
4,CC

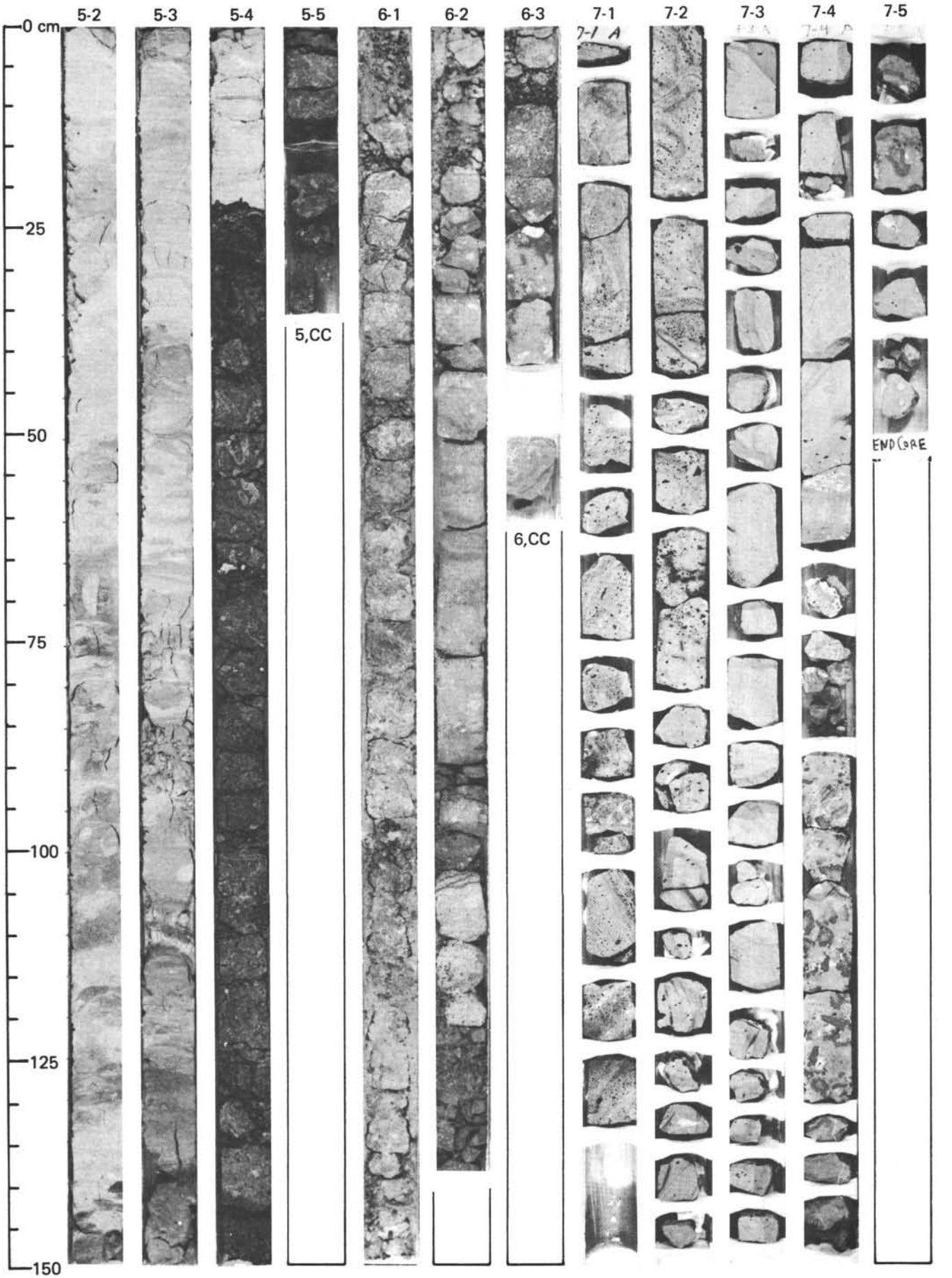
5-2
5-3
5-4
5-5
6-1
6-2
6-3
7-1
7-2
7-3
7-4
7-5
0 cm
25
50
75
100
125
150
5,CC
6,CC
END CORE


8-1
8-2
8-3
9-1
10-1
11-1
12-1
13-1
14-1
0 cm
25
50
75
100
125
150